HINTS OF UNIVERSALITY FROM INFLECTION POINT INFLATION

A Dissertation

by

SEAN DONOVAN DOWNES

Submitted to the Office of Graduate Studies of
Texas A&M University
in partial fulfillment of the requirements for the degree of

DOCTOR OF PHILOSOPHY

Chair of Committee,	Bhaskar Dutta
Committee Members,	Teruki Kamon
	Joseph Landsberg
	Christopher Pope
Head of Department,	George Welch

August 2013

Major Subject: Physics

ABSTRACT

This work aims to understand how cosmic inflation embeds into larger models of particle physics and string theory. Our work operates within a weakened version of the Landscape paradigm, wherein it is assumed that the set of possible Lagrangians is vast enough to admit the notion of a generic model. By focusing on slow-roll inflation, we examine the roles of both the scalar potential and the space of couplings which determine its precise form. In particular, we focus on the structural properties of the scalar potential, and find a surprising result: inflection point inflation emerges as an important — and under certain assumptions, dominant — possibility in the context of generic scalar potentials.

We begin by a systematic coarse graining over the set of possible inflection point inflation models using V.I. Arnold's ADE classification of singularities. Similiar to du Val's pioneering work on surface singularities, these determine structural classes for inflection point inflation which depened on a distinct number of control parameters. We consider both single and multifield inflation, and show how the various structural classes embed within each other. We also show how such control parameters influence the larger physical models in to which inflation is embedded. These techniques are then applied to both MSSM inflation and KKLT-type models of string cosmology.

In the former case, we find that the scale of inflation can be entirely encoded within the superpotential of supersymmetric quantum field theories. We show how this relieves the fine-tuning required in such models by upwards of twelve orders of magnitude. Moreover, unnatural tuning between SUSY breaking and SUSY preserving sectors is eliminated without the explicit need for any hidden sector dynamics. In the later case, we discuss how structural stability vastly generalizes — and addresses — the Kallosh-Linde problem. Implications for the spectrum of SUSY breaking soft terms are then discussed, with an emphasis on how they may assist in constraining the inflationary scalar potential.

We then pivot to a general discussion of the FLRW-scalar phase space, and show how inflection points induce caustics — or dynamical fixed points — amongst the space of possible trajectories. These fixed points are then used to argue that for uninformative priors on the space of couplings, the likelihood of inflection point inflation scales with the inverse cube of the number of e-foldings. We point out the geometric origin for the known ambiguity in the Liouville measure, and demonstrate of inflection point inflation ameliorates this problem.

Finally we investigate the effect of the fixed point structure on the spectrum of density perturbations. We show how an anomaly in the Cosmic Mircowave Background data — low power at large scales — can be explained as a by product of the fixed point dynamics.

DEDICATION

To my family.

ACKNOWLEDGEMENTS

I would like to acknowledge the guidance and support of my dissertation advisor Bhaskar Dutta. I am also grateful to the rest of my committee for their questions and courses over the years.

This work has also benefited greatly from my interactions with others: Rouzbeh Allahverdi, Paul Bruillard, Kuver Sinha and other members of the George P. and Cynthia Woods Mitchell Institute. My education in high energy physics and cosmology owes a great deal to discussions with JM Landsberg, Dimitri Nanopoulos, Nick Suntzeff and of course, my advisor.

In addition to these fine people I would like to acknowledge the enormous amount of support and perspective I gained from Bill Bassichis and Tatiana Erukhimova.

Special thanks are due to Sandi Smith and Beverly Guster for administrative guidance in the production of this dissertation. Thanks also to the Mitchell Institute and the United States Department of Energy for the funding which helped me complete this research.

Finally, a production note. This thesis is written in LaTeX2e with technical support from Roy Montalvo, Paul Bruillard and Jennifer Webster. Prose is typset in Palantino with the `MathPazo` package, and formulae are written with the help of the the `Euler` package. Much inspiration was drawn from Alexandru Scoropan's manuscript, "The Wild World of 4-Manifolds".

TABLE OF CONTENTS

LIST OF FIGURES

Page

CHAPTER I

INTRODUCTION

I.1 Invitation

As a paradigm, Inflationary Cosmology [1, 2, 3] attempts to explain the initial conditions for the Big Bang [4] model of cosmology. Given that even the simplest models of inflation reproduce features of the observed universe, *grosso moto*, it has become by far the most popular explanation for these phenomena.

In essence, inflation employs a condensate of scalar fields to generate an approximately de Sitter spacetime. Dynamical, cosmological matter typically breaks the de Sitter isometries down to spatial rotations. Therefore, one may view inflation as kin to the Higgs mechanism: time diffeomorphism invariance in the metric is restored by the fluctuations of the scalar field. From today's perspective, this would appear as an exponential expansion of distances in space. Physically, this symmetry restoration can be understood as an extremely slow evolution of the scalar condensate. Indeed, at its most extreme —the infrared limit of a scalar field at rest at a minimum of its potential with positive energy — inflation coincides with de Sitter space.

Attempting to theorize beyond Standard Model of Fundamental Interactions [5] has lead to a proliferation in the number of hypothetical scalar fields. These scalars are particularly abundant in string theory, where the so-called moduli fields of Calabi-Yau compactification can easily number in the thousands [6, 7]. It is unsurprising, then, that decades of investigation have led to an analogous zoo of inflationary scenarios. Many of these models have included smoking-gun signatures of novel, ultraviolet physics [8].

As of late, these models have been ruled out.

With the release of the Planck Collaboration's analysis [9], the universe appears to prefer the relatively anonymous scenario of a single, canonically normalized scalar field semi-classically rolling down a shallow potential. This fact has somewhat exacerbated complaints that Inflationary Cosmology is not sufficiently predictive and theoretically incomplete. While new theories have been put forth to address these issues [10, 11], it is not unreasonable to argue that such questions are moot until ultraviolet embeddings are better understood [12]. In spite of these concerns, the present work describes progress on this front. The uncertain identity of the inflaton is tied to uncertain knowledge of the initial conditions both of which are central themes of this dissertation.

Exceptional models may certainly exist. It may turn out that String Theory has a distinguished candidate inflaton. Future observations may motivate a particular model of inflation. At the time of writing, such is not our fortune. In the absence of experimental guidance, we choose to employ the assumption that our universe — and the inflationary model which best describes it

— is generic.

More precisely, we assume that inflation can be described by canonically normalized scalar fields under the influence of a suitably generic potential. The former condition is in line with the non-observation of primordial deviation from Gaussian statistics in the cosmic microwave background data. The latter condition is taken to mean generic within the set of smooth functions, *i.e.* no *a priori* correlation between coefficients in the Taylor series. In some sense, genericity of a scalar potential is analogous to the Wilsonian notion of naturalness of an effective field theory.

This approach immediately makes the problem with inflation manifest: there is a fine tuning. As we will argue, the observed sixty e-foldings of expansion has effectively made such a tuning mandatory in realistic models: either concretely in terms of couplings or vaguely in terms of initial conditions.

Our work localizes around the scenario of inflection point inflation, where a degenerate critical point of the scalar potential generates the phenomenologically observed expansion of space. Owning to the tuning between couplings, the inflection point scenario was simultaneously labelled "accidental" [13] and yet vigorously employed by model builders. In addition to developing a systematic framework, we shall argue inflection point inflation is favored amongst a landscape of possible models, a point that is (indirectly) supported by Monte Carlo calculations [14, 15].

I.2 Structural Stability and Universality

Critical points of a smooth function degenerate in universal ways. The simplest of these degenerations — including those relevant for inflection point inflation — were classified in V.I. Arnold's Singularity Theory [16]. This classification scheme is the mathematical structure beneath the physical phenomena of spontaneous symmetry breaking, a fact we shall exploit in this work. Indeed, the fine tuning required to bring two critical points together can be traced to the tuning required to bring a thermal system to its critical state. From this perspective, the scaling behavior of the spectrum of density perturbations generated during inflation is no surprise.

Physically, inflection point inflation occurs in the vicinity of a field configuration where the potential is locally cubic. Therefore the inflationary details of all models have some degree of universality. To make this statement precise consider a potential $\mathcal{V}$ in a scalar field ϕ which as a nearly degenerate critical point. By field redefinition, $\mathcal{V}$ may *always* be brought locally to a form,

$$\mathcal{V} = V_0 \left(1 + \lambda_1 \phi + \frac{\lambda_3}{3}\phi^3 + \cdots\right), \tag{I.1}$$

where $\lambda_1 \ll \lambda_3^{1/3}$. In such a case the universe expands by a factor $\exp N_e$, where the universal value of the number of e-foldings is

$$N_e \approx \frac{\pi}{2\sqrt{\lambda_1 \lambda_3}}.$$

Such cubic behavior is familiar from the study of a van der Waals gas: a maximum and a minimum degenerate at the critical end-point of the isotherm in a pressure/specific volume phase diagram. We may extend this analysis further. Having a third critical point degenerate means $\mathcal{V}$ is locally a quartic function. Such a degeneration would occur at the electroweak phase transition. Let us examine this case in detail.

For inflation, a simple quartic potential is not phenomenologically viable as it does not afford an exit to the standard big bang cosmology. A slight deviation from quartic to cubic behavior may be parametrized by α,

$$\mathcal{V} = V_0 \left(\frac{1}{4}\phi^4 + \alpha\phi^3 + \frac{27}{4}\alpha^4 + \cdots \right). \tag{I.2}$$

In the limit where $\alpha \to 0$, this form is also universal. Here the constant term is added to assure a phenomenologically valid solution: the minimum value of $\mathcal{V}$ is vanishingly small. As α grows, the universality of this result gets distorted, but the *structural* properties of $\mathcal{V}$ remain the same. In particular, the energy density during inflation scales with the distance between the inflection point and the local minimum. The universal quartic scaling for small α can pick up an "anomalous" dimension as α grows, which may eventually dominate and spoil the validity of the effective field theory. Arnold's classification scheme merely tells us that there exists a field redefinition which will bring the potential back to (I.2), at the expense of having non-canonical kinetic terms in the Lagrangian.

This is a peculiar sort of flow in the space of couplings, were the boundary conditions change rather than the energy scale. For the case of flow in α, the stability structure of the theory, however, remains intact. This is not generally true. Flow towards negative λ_1 in (I.1) will break the cubic point into a maxima and minima.

In this dissertation, we study this phenomena systematically in the context of inflation. We derive both universal properties and a classification of inflection point models based on the stability structures alluded to above. These structures are generic and allow for an organized way to discuss the embedding of inflation into string theory or particle physics models. This new clarity deepens physical insight, and we describe new results based this new perspective. We also study how the trajectories behave under flow in the space of couplings. In turn, this leads to a flow in the space of effective Lagrangians for the cosmological perturbations. We finish our discussion by describing some observational implications in this framework.

I.3 Selections from the Literature

Inflation dates back to the work of Starobinsky [17], where the idea of a universe born from a de Sitter state was shown to be consistent with a nearly scale-invariant spectrum of perturbations. The idea that exponential expansion could resolve a number of problems with big bang cosmology was really put together first by Guth [1]. This work was quickly revised in [2, 3]. A number of scenarios were envisioned to explain the gravity-scalar system. Notable amongst these was Chaotic Inflation [18], which took a first stab at the issue of initial conditions by suggesting that

a sufficiently large fluctuation in vacuum expectation value (VEV) of the scalar field could exist near the Planck scale. Hyrbid inflation [19], was an alternative proposal which took aim at explaining the end of inflation. Here a second scalar field was employed as a spectator, and inflation ended with the phase transition induced decay of this spectator or waterfall field condensate. All of these models attempted to explain the required sixty or so e-foldings of expansion required by observations. A curious fact about such models is that the duration of inflation depended primarily on the excursion in field space, rather than the actual energy scales. This lead naturally to the issue of transplanckian field VEVs, which made the effective field theory models of such physics difficult to interpret.

Inflection point inflation was devised as a simple means of embedding inflation into larger physical models. While fine tunings are problematic in physics, a tuning in the potential was at least a well defined problem, easy to postulate and under parametric control.

So far all of these models of inflation have invoked details of the scalar potential. Changing the kinetic terms of the Lagrangian can also induce a period of quasi-de Sitter expansion [20]. D-brane dynamics, replete with their Dirac-Born-Infeld (DBI) action were used to study inflation in [21]. More exotic scenarios from the kinetic sector were also considered, notably Ghost Inflation [22]. Aside from finding novel scenarios or embeddings into string models, these models primarily sought to construct new observables. Non-canonical kinetic terms have the potential to produce a spectrum of fluctuations that deviates from that expected by Gaussian statistics in a measurable way. Much work has gone into observing and quantifying such deviations [23]. Maldaecena's seminal calculation [24] is the classic reference for nongaussianity.

There are, of course, other ways to arrange for this. As demonstrated with hybrid inflation, allowing for multifield dynamics can open new possibilities. The Curvaton mechanism [25, 26, 27] allowed the adiabatic perturbations generated during inflation to be transferred to spatial curvature via a second, curvaton field. Significant nongaussianity could be generated by such a transfer.

More recent develops in inflation have focused on systematizing the various results and zoo of inflationary models. The δN formalism allows one to compute correlators of the primordial curvature perturbation in terms of the scalar field correlators. For a particularly crisp treatment — and the original references — see Ref. [28]. Effective field theory techniques where first systematically applied to inflation in Ref. [29] and slightly generalized by Weinberg [30].

In spite of the large number of new observables — and the possible window into near Planck-scale physics, results from Planck suggest that nature insists on a very nearly Gaussian distribution of fluctuations. Many of these phenomenologically interesting models have now been ruled out.

Baumann's lectures [31] comprise an extensive and accessible introduction to inflation. Weinberg's textbook [32] is a fairly complete introduction to modern cosmology.

I.4 Preview

This dissertation is arranged as follows. We review the basics of inflation in chapter II. We pay particular attention to the attractor dynamics while reviewing a number of the different inflationary scenarios. We close the chapter by a discussion of linear perturbations of the gravity-scalar system.

Our discussion of genericity amongst inflationary models is framed by a discussion of the landscape of string vacua in chapter III. We review the basics of Calabi-Yau compactification, the resulting effective supergravity models and the possible realization of meta-stable de Sitter vacua. We close with a brief discussion of Weinberg's proposed explanation of the small cosmological constant [33].

In Chapter IV we begin our classification program in earnest. Studying the critical points of scalar potentials as functions of the space of couplings allows us to classify the structural classes of inflection point inflation using Arnold's ADE classification of singularities. This classification is our first major result and lays the foundation for the rest of our analysis. It is based primarily on Ref. [34].

Chapter V looks at how inflation embeds into supersymmetry particle physics through a pair of case studies. First, we apply these techniques to the MSSM-inflation scenario. This new approach to embedding inflation in supersymmetric quantum field theories eliminates technically unnatural tuning in the SUSY breaking sector while preserving weak scale supersymmetry. The scale of inflation comes entirely from the superpotential, which improves the required tuning by nearly twelve orders of magnitude. This was first discussed in Ref. [35]. Second, we discuss how the stability classes dictate how details of the inflationary scalar potential embed into the SUSY breaking soft-terms in the context of a KKLT moduli stabilization scenario, which was also dealt with in Ref. [34].

Chapter VI investigates the effects of inflection points in phase space. Expanding on the discovery in Ref. [36], we show how inflection points can generate caustics amongst the set of trajectories. These caustics act as inflationary fixed points and are used to bolster the attractor-as-predictor argument for inflation. We extend the ensemble of universes to include all possible couplings in the potential, which leads to an analytic derivation of an inverse cubic power law for the likelihood of inflation observed by a number of Monte Carlo computations. This is based on the work in Ref. [37].

In Chapter VII we employ properties of the fixed point dynamics of inflection point inflation to explain an anomaly in the power spectrum of the CMB. The low power observed at the lowest ($\ell \lesssim 20$) angular modes on the sky can be explained by a temporary deviation from slow-roll which generally arises as the inflaton approaches the inflection point. Importantly, this deviation scales with the structural parameters discussed in Chapter IV. This chapter is based on our work in Ref. [38]. Finally, we draw our conclusions in Chapter VIII.

CHAPTER II

INFLATIONARY COSMOLOGY

We review the basics of inflation and establish notation that will be used throughout this work. A more extensive treatment can be found in either of [31, 32].

II.1 Scalar Fields in Cosmology

II.1.1 Dynamics

The dynamics of the early universe are assumed to be determined by a canonical scalar field minimally coupled to the metric. The action for this theory is

$$S = \frac{1}{2}\int d^4x\,\sqrt{-g}\,(R + g^{\mu\nu}\partial_\mu\phi\partial_\nu\phi - 2\mathcal{V})\,.$$

The spacetime metric consistent with the cosmological principles of spatial uniformity is,

$$ds^2 = c^2dt^2 - a^2(t)\left(\frac{dr^2}{1-kr^2} + r^2d\theta^2 + r^2\sin^2\theta d\phi^2\right). \tag{II.1}$$

It is often referred as the **Friedmann-Lemaître-Robertson-Walker (FLRW) metric**. The single, dynamical degree of freedom is the scale factor, a. The parameter k takes values ±1 or zero and is the normalized spatial curvature. Spatial uniformity restricts the dynamics to a changing notion of distance. The Euler-Lagrange equations which minimize S are traditionally written in terms of the **Hubble parameter**, $H = \dot{a}/a$. The temporal equation is a constraint,

$$H^2 + \frac{k}{a^2} = \frac{1}{3}\left(\dot{\phi}^2 + \mathcal{V}\right), \tag{II.2}$$

whereas the spatial equations uniformly represent the dynamics of the scale factor,

$$\dot{H} = -\frac{1}{2}\dot{\phi}^2 + \frac{k}{a^2}. \tag{II.3}$$

The field equation for ϕ itself is

$$\ddot{\phi} + 3H\dot{\phi} + \mathcal{V}_\phi = 0. \tag{II.4}$$

The generalization of these equations to multiple fields is straight forward.

There are two (partial) gauge choices which simplify calculations. Both involves reparametrization of time. The first is so-called **conformal time**,

$$t \mapsto \eta(t) =_{\text{def}} \int^t \frac{dt'}{a(t')}.$$

The second is

$$t \mapsto N(t) =_{\text{def}} \log a(t),$$

the use of which is sometimes referred to as the **gradient expansion method**. In general, for a smooth function of time $q(t)$,

$$\frac{dq}{dt} = a\frac{dq}{d\eta} = H\frac{dq}{dN}.$$

Let us rewrite (II.4) in terms of these two reparametrizations of time. In conformal time we have,

$$\phi^{\star\star} + 2aH\phi^{\star} + V_{\phi} = 0, \tag{II.5}$$

where superscript stars represent derivatives with respect to η. In terms of N we have

$$\phi'' = -3(1 - \frac{1}{6}\phi'^2)\left(\phi' + \frac{\partial \log V}{\partial \phi}\right), \tag{II.6}$$

where primes denotes derivatives with respect to N. Note also that the Hubble parameter in this coordinates is given by

$$H^2 = \frac{a^2\phi^{\star 2} + 2V}{6} = \frac{V}{3(1 - \frac{1}{6}\phi'^2)}. \tag{II.7}$$

II.1.2 Accelerated Expansion

Inflation is defined to be accelerated expansion of spacetime. In terms of the FLRW scale factor, this means positive $\ddot{a}$. Traditionally, it is computed in terms of the **deceleration parameter** q,

$$(-q) = \frac{\ddot{a}a}{\dot{a}^2} = 1 - \frac{\dot{H}}{H^2}, \tag{II.8}$$

In terms of N, accelerated expansion occurs for any $|\phi'| < \sqrt{2}$. We now demonstrate how the stability of spatial flatness depends on the sign of q. For a given value of H, the critical energy density — that energy density at which k vanishes — is $\rho_C = 3H$. The magnitude of the curvature of space is given by the quantity

$$\Omega_k =_{\text{def}} \frac{k}{a^2\rho_C} = \frac{k}{3a^2H^2}.$$

Let us compute Ω_k,

$$\Omega_k' = -2\frac{k(a'H + aH')}{(aH)^3} = 2q\Omega_k.$$

Therefore

$$\Omega_k \propto e^{2qN}. \tag{II.9}$$

As made explicit in (II.9), accelerated expansion forces spatial curvature decays exponentially.

II.1.3 Attractor Dynamics

The attractor properties of the gravity-scalar system is was discussed in detail in Salopek and Bond's work [39], as well as Liddle, *et. al.* [40]. While some of these technical details were known — especially to Kofman [41] — to the best of our knowledge they were first presented in this manner in [37]. In any case, there appears to be some confusion in the community, so we wish to stress one important fact:

The slow-roll trajectory can be an attractor regardless of whether the universe is inflating or not.

We now qualify "can" and see how this comes about. To manifest the attractor dynamics, consider first the case of a single, canonical scalar field, ϕ. With simple algebra, the flow equation (II.6) reads,

$$\phi'' = \frac{1}{2}\left(\phi' + \sqrt{6}\right)\left[\phi' + \frac{\partial \log \mathcal{V}}{\partial \phi}\right]\left(\phi' - \sqrt{6}\right). \tag{II.10}$$

This second order, nonlinear differential equation has two singular solutions, where

$$\phi' = \pm\sqrt{6}.$$

These solutions are unphysical; our assumptions about monotonicity of a break down since H vanishes here. Despite the singularity in (II.7), configurations with ϕ' very close to $\pm\sqrt{6}$ can be considered to be kinetic energy dominated.

Now the full equation (II.10) is solved easily if $\kappa =_{\text{def}} -\mathcal{V}_\phi/\mathcal{V}$ is a constant. In this case (II.10) becomes,

$$\phi'' = (\phi' - \sqrt{6})(\phi' - \kappa)(\phi' + \sqrt{6}),$$

which is a *first order* differential equation in ϕ'. A third singular solution appears, $\phi' = \kappa$, in which

$$\phi = \kappa N + \text{constant}, \quad \phi = \pm\kappa\sqrt{6} + \text{constant}.$$

All other solutions interpolate between these three. As it turns out, two are repulsor solutions, and one is an attractor. For a general first order differential equation with three constants $A < B < C$,

$$x' = (x - A)(x - B)(x - C),$$

all trajectories started between A and C will exponentially approach B. Other trajectories will run off to $\pm\infty$.

κ may be a constant either if the potential is an exponential, $\mathcal{V} \propto e^{\kappa\phi}$ or, if $\mathcal{V}_\phi/\mathcal{V}$ is very close to zero. The latter is clearly the case of interest, for then $-\sqrt{6} < \kappa < \sqrt{6}$, which implies that

$$\phi' = -\frac{\mathcal{V}_\phi}{\mathcal{V}} \tag{II.11}$$

is the attractor trajectory.

"Very close to zero" can be qualified by recursively checking the solution. If $\kappa \approx 0$, then the RHS of (II.10) vanishes. This requires that the LHS vanish also, which amounts to the condition

$$\frac{\mathcal{V}_{\phi\phi}}{\mathcal{V}} - \left(\frac{\mathcal{V}_{\phi}}{\mathcal{V}}\right)^2 \approx 0. \tag{II.12}$$

This condition is the precise statement of what is usually meant by the "slow-roll conditions". An alternative definition in terms of the Hubble parameter can be defined similarly, although with somewhat reduced precision.

While we explore various scenarios in the next section, these equations represent fundamental idea behind inflation: kinetic energy is redshifted with expansion, slowing the towards potential energy dominance, *i.e.* de Sitter space. The conditions on $\mathcal{V}$ for this to happen are given in (II.11). Such behavior is generic, as either the potential may have small derivatives or an extremely large value, which is certainly easy to arrange for any polynomial in ϕ.

The attractor dynamics of inflation are important since we have little technical understanding of the earliest moments of the universe. Nevertheless, a large fraction of initial conditions appear to give rise to a period of inflation. There is, however, a wrinkle. Qualifying large has proven difficult, since we cannot access an ensemble of universes for a suitable experiment. The measure on the space of possible universes — to the extend that such a thing is sensible — is not well understood. Therefore, associating attractor dynamics with predictability may be premature. We shall return to this point in some detail in Chapter VI. In the meantime, we investigate different ways inflation can arise.

II.2 Some Inflationary Scenarios

II.2.1 Old Inflation

Old inflation models simply allow the inflaton to be at rest at some reasonably short-lived metastable vacuum, generating inflation staying put. Since de Sitter space is unstable to vacuum decay, the model involved tunnelling into the present, nearly Minkowski spacetime. Like a first order phase transition, inflation would end when bubbles of non-expanding universe percolated through spacetime.

Percolation never happens in an exponentially expanding background, although it not required *a priori*. Were our universe to be a bubble adrift in an exponentially expanding background, we might never be the wiser. From similiar arguments old inflation has found new traction in the context of eternal inflation [42, 43]. There are even attempts to construct cosmological observables along these lines [44].

In any case, the power spectrum of perturbations generated during a period of false-vacuum inflation should be scale invariant. Observations by WMAP [45] and more recently Planck [9]

have put strong constraints on the spectrum, which rules out exact scale invariance at the 5σ level in favor of a slightly tilted spectrum favoring longer wavelength modes. Such deviations are generic to dynamical models of inflation slow-roll inflation.

II.2.2 Chaotic Inflation

For our purposes chaotic inflation is synonymous with large excursion, slow-roll inflation. Although depending on the scalar potential, the initial conditions have to be chosen carefully to ensure enough expansion occurs. The main thrust of the original work [18] on chaotic inflation was to explain these initial conditions.

Consider a simple quadratic potential,

$$\mathcal{V} = \frac{1}{2} m^2 \phi^2. \tag{II.13}$$

The slow-roll trajectory (II.11) is,

$$\phi' = -\frac{2}{\phi}, \tag{II.14}$$

which satisfies the slow-roll conditions (II.12) when $\phi \gg 1$.

The number of e-foldings of inflation can be computed by integrating (II.14),

$$-\int_{\phi_i}^{\phi_f} \frac{\phi d\phi}{2} = \int_0^{N_e} dN,$$

which gives

$$N_e = \frac{1}{4}\left(\phi_i^2 - \phi_f^2\right). \tag{II.15}$$

Inflation ends when $\phi' = -\sqrt{2}$, or

$$\sqrt{2} = \frac{2}{\phi} \Rightarrow \phi = \sqrt{2}.$$

So a phenomenologically viable fifty e-foldings would requires that

$$200 = \phi_i^2 - 2 \Rightarrow \phi_i \approx 14.$$

Such a number would appear to be reasonable until units are replaced. Set the mass scale of ϕ to be be Λ, and let $m = \mu\lambda$. Using the Planck scale as an upper bound to the energy density,

$$M_P^4 = \frac{N_e^2}{2} \mu^2 \Lambda^4. \tag{II.16}$$

If Λ is near the Planck scale — which seems to be a reasonable requirement for the earliest moments of the universe, then μ has to be fine-tuned to one part in N_e.

Particle physics has a number of techniques for dispatching fine tuning problems. For example, a quartic potential whose coupling is kept small by an shift symmetry could lead to a viable potential. Despite such field theoretic mechanisms, attempts to embed chaotic inflation models in to supergravity or string theory have been stymied by higher dimensional, Planck suppressed operators. They typically spoil the slow-roll conditions (II.12) by contributing to the scalar potential in uncontrollable ways. This has become known as the η-problem [46]. Although there has been progress on this front [47, 48].

But there is more. This is the minimal tuning required of the potential to allow for fifty e-foldings of inflation. One must also explain how the field managed to start at a VEV near the Planck scale. Linde's original work remarks that this can simply happen at some random point in spacetime owning to the potentially violent effects of Planckian quantum dynamics. In other words, the universe just needs one large fluctuation among a huge ensemble of possibilities to inflate which, although rare, is certainly possible. This perspective is amplified in Kofman, Linde, and Mukhanov [49], but no quantitative calculations are given. Other attempts at such calculations have been ambiguous, and some have given precisely the opposite answer to [50]! We return to these arguments in detail in Chapter VI.

In short, there are two tunings to resolve, the couplings and the initial conditions. The former is a tractable problem, the latter is considerably less so.

II.2.3 Inflection Point Inflation

Where chaotic inflation solved the slow-roll conditions (II.12) at a large value of $\mathcal{V}$, inflection point inflation solves these conditions by assuming the first and second derivatives of the potential vanish at a particular field value, $\phi_\star$. In short, $\phi_\star$ is a degenerate, real critical point of $\mathcal{V}$.

The slow-roll trajectory has vanishing kinetic energy at a precisely degenerate critical point, so it may slow the field down considerably and generate a sizable amount of inflation over a short distance in field space. This is in stark contrast to the case of chaotic inflation discussed above, and helps to alleviate the problem of initial conditions, since the field must only start somewhere above the inflection point.

Near the inflection point, the inflaton potential has the universal form,

$$\mathcal{V} = V_0 \left(1 + \lambda_1 \phi + \frac{\lambda_3}{3}\phi^3\right) + \mathcal{O}(\phi^4), \tag{II.17}$$

since any ϕ^2 can be removed by a shift. Here λ_1 must be very small; it is the same qualitative tuning as in the mass parameter of (II.13). Once again we can compute the number of e-foldings,

$$N_e = -\int_{\phi_i}^{\phi_f} d\phi \frac{\mathcal{V}}{\mathcal{V}_\phi}.$$

For simplicity, let us assume that ϕ initially starts at the inflection point. Then the minimal

number of e-foldings will be

$$N_e = -\int_0^{\phi_f} d\phi \frac{1 + \lambda_1 \phi + \frac{\lambda_3}{3}\phi^3}{\lambda_1 + \lambda_3 \phi^2}.$$

If λ_1 is indeed small, this integral is dominated by the contribution near the inflection point, *i.e.* where $\phi \approx 0$. Therefore,

$$N_e = -\int_0^{\phi_f} d\phi \frac{1}{\lambda_1 + \lambda_3 \phi^2}, \tag{II.18}$$

which is approximately,

$$N_e \approx \frac{\pi}{2\sqrt{\lambda_1 \lambda_3}}. \tag{II.19}$$

Notice that fifty e-foldings of inflation require that λ_1 is indeed quite small.

Inflection point inflation has been studied extensively in the context of string theory and particle physics models. This is largely because models are easy to construct. Blind application of the slow-roll conditions in this context have lead to a number of problems which we resolve in this work. In the following chapters, we shall also discuss how inflection point inflation helps soften the problem of initial conditions in cosmology, how it is in solid agreement with observations and will make scenario specific predictions that can be tested in the CMB data.

II.3 Cosmological Perturbation Theory

At scales below $100h^{-1}$ Mpc, fluctuations about the FLRW background are statistically significant at around the ten percent level [51]. Below this scale, the distribution of matter in the universe is self similar. These fluctuations are thought to have been sourced by primordial fluctuations in the energy density, which the theory of inflation seeks to explain. Statistical studies of these fluctuations have driven much of modern Cosmology, so we spend some time to develop their main theoretical framework: **cosmological perturbation theory**.

II.3.1 The General Framework

So far a cosmology has been specified by the FLRW scale metric, $g_{\mu\nu}$ and two fluid parameters ρ and p. To study perturbations around them, we write the metric as,

$$g_{\mu\nu} = \bar{g}_{\mu\nu} + h_{\mu\nu},$$

where $\bar{g}_{\mu\nu}$ is the background FLRW metric (II.1), and $h_{\mu\nu}$ is referred to as its perturbation. We similarly write the stress energy tensor as

$$T_{\mu\nu} = \bar{T}_{\mu\nu} + \delta T_{\mu\nu}.$$

One difficulty in this analysis is the differomorphism invariance of the action, S. Not all perturbations of the metric or matter will be physically distinct from the background. Fixing a gauge

removes this problem at two costs. First, gauge covariant notation may be simpler to work with. Second, intuition in one gauge may not hold in another gauge, and different gauge choices are useful for different purposes or perspectives. Since physical observables are gauge invariant, one must take care to define and work with gauge invariant variables such as those introduced by Bardeen [52].

The physical perturbation of spacetime is an admixture of a metric and matter perturbation. "How much" of "which part" is a matter of perspective; it depends on choice of gauge. This can be confusing, so we shall attempt to be as organized as possible about the physics. To that end we employ the **Arnowitt-Deser-Misner** (ADM) formalism [53], which expand the full metric $g_{\mu\nu}$ as,

$$ds^2 = \mathfrak{N}^2 dt^2 - \gamma_{ij}\left(dx^i + \mathfrak{N}^i dt\right)\left(dx^j + \mathfrak{N}^j dt\right). \tag{II.20}$$

Here $\mathfrak{N}$ and $\mathfrak{N}^i$ are called the **lapse function** and **shift vector**, respectively. They can be viewed as Lagrange multipliers that impose constraints on the dynamics, although they are both functions of spacetime coordinates.

The main idea is to consider space on fixed time slices so that the Hamiltonian formalism of dynamics can be applied. To that end the four-dimensional Einstein-Hilbert action splits in terms of the three-dimensional intrinsic and extrinsic curvatures,

$$S_{EH} = \frac{1}{2}\int d^4x\, \frac{1}{N}\left[N^2 R^{(3)} + E_{ij}E^{ij} - E^2\right], \tag{II.21}$$

where the extrinsic curvature is $K_{ij} = E_{ij}/N$, so $K = E/N$ and

$$E_{ij} = \frac{1}{2}\dot{\gamma}_{ij} - \nabla_{\{i}N_{j\}}. \tag{II.22}$$

$$E = \gamma^{ij}E_{ij}. \tag{II.23}$$

The equations of the lapse and shift are,

$$R^{(3)} - K_{ij}K^{ij} + K^2 = 2T_{00}, \tag{II.24}$$

$$\nabla_i\left(\gamma^{im}K_{mj} - \delta^i_j K\right) = \nabla^i T_{ij}, \tag{II.25}$$

respectively. Note that the lapse constraint (II.24) would be the Friedmann constraint in the unperturbed metric.

Let us now focus on a single, canonical scalar field. In keeping with the spirit of the ADM formalism, we now fix a gauge to port all the perturbed dynamics into γ_{ij} by using the so-called **comoving gauge**. We take $\delta\phi$ to vanish, and γ_{ij} to be

$$\gamma_{ij} = a^2\left[(1 + 2\mathcal{R})\delta_{ij} + q_{ij}\right],$$

where q_{ij} is transverse-traceless, and $\mathcal{R}$ is the **curvature perturbation**.

The standard [24, 31] thing to do is to solve the constraint equations to each order in perturbation theory by writing

$$\mathfrak{N} = 1 + \mathfrak{n}, \quad \mathfrak{N}^i = \partial^i \psi + N_T^i,$$

where N_T^i is transverse, *i.e.* $\partial_i N_T^i$ vanishes. Here each of $\mathfrak{n}$, ψ and N_T^i are formally expanded about zero. For example,

$$\mathfrak{n} = \epsilon \mathfrak{n}^{(1)} + \epsilon^2 \mathfrak{n}^{(2)} + \epsilon^3 \mathfrak{n}^{(3)} \cdots,$$

where ϵ plays double duty as the formal "small" bookkeeping parameter which counts the order of perturbations and the order of $\mathcal{R}$-dependence. Clearly, this is an approximation scheme which requires $\mathcal{R}$ to remain small.

II.3.2 The Linear Perturbations

To study the linear perturbations, it remains to solve these constraint equations and plug into the action at the order ϵ^2. After some work — detailed in [31] — we find,

$$S_{\mathcal{R}} = \frac{1}{2} \int d^4x \, a^3 \phi'^2 \left(\dot{\mathcal{R}}^2 - \frac{1}{a^2} \delta^{ij} \partial_i \mathcal{R} \partial_j \mathcal{R} \right). \tag{II.26}$$

To apply our intuition from Minkowski quantum field theory, we push to the conformal gauge,

$$S_{\mathcal{R}} = \frac{1}{2} \int d^4x \, a^2 \phi'^2 \left(\mathcal{R}^{\star 2} - \delta^{ij} \partial_i \mathcal{R} \partial_j \mathcal{R} \right). \tag{II.27}$$

The Euler-Lagrange equations for this action are,

$$(a\phi')^2 \left(\mathcal{R}^{\star\star} + 2H \left[1 + \frac{\phi''}{\phi'} \right] \mathcal{R}^{\star} - \triangle \mathcal{R} \right) = 0.$$

The $\mathcal{R}^\star$ term can be eliminated by opting for a canonical normalization of (II.26). A standard Liouville transformation

$$\mathcal{R} \to \mathcal{Q} = a\phi' \mathcal{R},$$

brings us to the field equation for the Mukhanov-Sasaki variable $\mathcal{Q}$,

$$\mathcal{Q}^{\star\star} - \left(\triangle + \frac{z^{\star\star}}{z} \right) \mathcal{Q} = 0. \tag{II.28}$$

Here $z = a\phi'$. In terms of ϕ,

$$\mathcal{Q}^{\star\star} - \left(\triangle + (aH)^2 \left[2(1 - \frac{1}{2}\phi'^2)(1 + \frac{\phi''}{\phi'}) + (\frac{\phi''}{\phi'} + \left(\frac{\phi''}{\phi'} \right)' + \frac{\phi''^2}{\phi'^2}) \right] \right) \mathcal{Q} = 0. \tag{II.29}$$

Let use define the **slow-roll parameter**,

$$\Xi =_{\text{def}} \frac{\phi''}{\phi'}, \tag{II.30}$$

so that (II.29) becomes,

$$\mathcal{Q}^{\star\star} - \left(\triangle + (aH)^2\left[(2-\phi'^2+\Xi)(1+\Xi)+\Xi'\right]\right)\mathcal{Q} = 0. \tag{II.31}$$

Alternatively, we may employ the **flat gauge**, where $h_{\mu\nu}$ vanishes. In this case the quadratic action for the scale fields is

$$S_{\delta\phi} = \frac{1}{2}\int d^4x\, a^2\left(\delta\phi^{\star 2} - |\vec{\nabla}\delta\phi|^2 - a^2 V_{\phi\phi}\delta\phi^2\right).$$

Again, opting for canonical normalization leads to the variable,

$$\delta\phi \to \psi = a\delta\phi.$$

So we find,

$$\psi^{\star\star} - \left(\triangle + (aH)^2[2 - \frac{V_{\phi\phi}}{H^2} - \frac{1}{2}\phi'^2]\right)\psi = 0,$$

which becomes,

$$\psi^{\star\star} - \left(\triangle + (aH)^2[2 - 3(1-\frac{1}{6}\phi'^2)\frac{V_{\phi\phi}}{V} - \frac{1}{2}\phi'^2]\right)\psi = 0. \tag{II.32}$$

II.3.3 The de Sitter Limit

In the de Sitter limit, both (II.31) and (II.32) reduces to the same form,

$$\psi^{\star\star} - \triangle\psi - 2(aH)^2\psi = 0.$$

Note that in this limit H is constant and

$$\eta = \int^t e^{-H\tau}d\tau = \frac{1}{aH}. \tag{II.33}$$

Fourier transforming ψ,

$$\psi = \int \frac{d^3k}{(2\pi)^3}\left(a_{\vec{k}}\psi_k e^{i\vec{k}\cdot\vec{r}} + a^\dagger_{\vec{k}}\overline{\psi}_k e^{-i\vec{k}\cdot\vec{r}}\right),$$

we find

$$\psi_k^{\star\star} + \left(k^2 - \frac{2}{\eta^2}\right)\psi_k = 0.$$

Solutions to this equation can be written in terms of spherical Hankel functions,

$$\psi_k(k\eta) = \frac{k\eta}{\sqrt{2k}}\left(Ah_1^{(1)}(k\eta) + Bh_1^{(2)}(k\eta)\right).$$

A feasible quantum vacuum for the earliest moments of the universe should only include outgoing waves, so B must vanish. Peculiar effects may persist if this is not the case [54, 55, 56, 57], some of which are still not entirely ruled out observationally. Also, we have include the normalization factor $\sqrt{2k}$ in the mode functions to ensure that

$$[a_{\vec{k}}, a^{\dagger}_{\vec{k}}] = \delta^{(3)}(\vec{k}\vec{k}'). \tag{II.34}$$

Now,

$$h_1^{(1)}(k\eta) = \frac{e^{ik\eta}}{(k\eta)^2}(1 - ik\eta), \quad h^{(2)} = \overline{h^{(1)}}.$$

At late times,

$$|\psi_k|^2 = a^2 \frac{H^2}{k^3},$$

where we have applied (II.33). In terms of our original variables,

$$|\delta\phi_k|^2 = \frac{H^2}{k^3}.$$

Similarly,

$$|\mathcal{R}|^2 = \frac{1}{\phi'^2}\frac{H^2}{k^3}.$$

Since we have defined properly normalized mode operators $a_{\vec{k}}$ and $a^{\dagger}_{\vec{k}'}$, an immediate consequence of (II.34) is the traditional result for de Sitter perturbations

$$\boxed{\langle \mathcal{R}_{\vec{k}}(t)\mathcal{R}_{\vec{k}'}(t)\rangle = \frac{(2\pi)^3}{\phi'^2}\frac{H^2}{k^3}\delta(\vec{k}+\vec{k}').} \tag{II.35}$$

II.3.4 Deviations from de Sitter

Owing to the large number of e-foldings, the physical power spectrum will differ from (II.35) only slightly. These deviations in terms of both ϕ' and the Ξ parameter. Since (II.31) can similarly be solved in terms of spherical Hankel functions, one can follow precisely the same steps as in Sec. II.3.3 to find the slow-roll correlators. We close this chapter by establishing some conventional notation to parametrize and interpret such results.

The **power spectrum of density perturbations**, $\mathcal{P}_{\mathcal{R}}(k)$ is defined by the relation,

$$\langle \mathcal{R}_{\vec{k}}(t)\mathcal{R}_{\vec{k}'}(t)\rangle = \mathcal{P}_{\mathcal{R}}(k)(2\pi)^3\delta(\vec{k}+\vec{k}'). \tag{II.36}$$

The **power spectrum normalization**, $\Delta^2_{\mathcal{R}}$ is defined by

$$\Delta^2_{\mathcal{R}}(k) =_{\text{def}} \frac{k^3\mathcal{P}_{\mathcal{R}}(k)}{(2\pi)^2}.$$

These computational acrobatics are meant to clarify observations, as the real space statistical variance of density perturbations can then be written as a Fourier transform,

$$\langle \mathcal{R}\mathcal{R} \rangle \propto \int_0^\infty d\log k\, \Delta^2_{\mathcal{R}}(k).$$

Notice that the angular degrees of freedom have been integrated over.

The **spectral index** of density perturbations is defined to be

$$n_s = 1 - \frac{d\log \Delta^2_{\mathcal{R}}}{d\log k},$$

so that in the de Sitter case $n_s = 1$. Slow-roll inflation that n_s is typically only slightly smaller than unity. Given that observations peg n_s near 0.96 [9], its prediction is considered a success of inflation.

We now briefly consider $\mathcal{R}$ away from the de Sitter limit. From (II.31), the Fourier components of the Mukhanov-Sasaki variable $\mathcal{Q}$ can also be written in terms of spherical Hankel functions,

$$\mathcal{Q}_k = \frac{x h^{(1)}_\nu(x)}{\sqrt{2k}},$$

with

$$x =_{\text{def}} k(\eta - \eta_\star). \tag{II.37}$$

Here $\eta_\star$ is the conformal time when the perturbations relevant for the CMB left the horizon. Similarly, it is convenient to define the parameter

$$u =_{\text{def}} aH(\eta - \eta_\star) \tag{II.38}$$

To maintain the Minkowski-like vacuum with no "outgoing" modes, the coefficient of $h^{(2)}_\nu$ is set to zero.

The index ν is determined from (II.31),

$$\nu_\pm = -\frac{1}{2} \pm \frac{1}{2}\left(1 + 4u^2\left[(1+\Xi)(2+\Xi-\frac{1}{2}\phi'^2) + \Xi'\right]\right)^{1/2}. \tag{II.39}$$

Since $h^{(1)}_{\nu_\pm}$ are complex conjugates of one another, and we are only interested in the modulus, we take $\nu = \nu_+$ unless otherwise specified. In this case, the de Sitter limit implies $\nu = 1$. We may then compute the normalization of the power spectrum, converting from $\mathcal{Q}$ to $\mathcal{R} = \mathcal{Q}/a\phi'$,

$$\Delta^2_{\mathcal{R}} = k^3 \left| \frac{x h^{(1)}_\nu(x)}{a\phi'\sqrt{2k}} \right|^2.$$

Let us use our conventions to convert k to x,

$$k \to \frac{x}{\eta - \eta_\star} \to x(uaH),$$

so that $\Delta^2_{\mathcal{R}}$ becomes,

$$\boxed{\Delta^2_{\mathcal{R}} = x^4 \left| h^{(1)}_\nu(x) \right|^2 \left(\frac{(uH)^2}{\phi'^2} \right).} \tag{II.40}$$

Since we are interested in modes on the largest scale, $x \ll 1$, we can approximate the Hankel Functions,

$$\begin{aligned} |h^{(1)}_\nu(x)|^2 &\to x^{-2\nu-2}, \quad \nu > 0, \\ |h^{(1)}_\nu(x)|^2 &\to x^{-2\nu}, \qquad \nu < 0. \end{aligned}$$

Therefore, if $\nu = 1 + \varpi$,

$$\Delta^2_{\mathcal{R}} = x^{-2\varpi} \left(\frac{(uH)^2}{\phi'^2} \right),$$

which means that the spectral index,

$$n_s = 1 - 2\varpi.$$

Let us compute ϖ from (II.39). For small ϕ'^2 and Ξ, $u \approx 1$, so to first order in these parameters,

$$\nu = 1 + \frac{1}{3} \left[(\Xi - \frac{1}{2}\phi'^2) + \Xi' \right],$$

so

$$\boxed{\varpi = \frac{1}{3} \left[(\Xi - \frac{1}{2}\phi'^2) + \Xi' \right].} \tag{II.41}$$

Note that the traditionally presented approximation,

$$n_s \sim 1 - 2\eta - 4\epsilon,$$

comes from

$$\Xi = \eta - 2\epsilon,$$

but does not quite represent the correct limit of (II.41), as $\frac{1}{2}\phi'^2 \to \epsilon$ as $\Xi \to 0$.

Let's close this chapter by illustrating the properties of $\Delta_{\mathcal{R}}$ for various ν. In Fig. II.1, we see the transitioning between a redshifted and a blueshifted spectrum occurs as ν passes through unity.

For large k, the normalization of the power spectrum is parabola, $\Delta^2_{\mathcal{R}\,dS} \propto 1 + k^2$. The minimum of this quantity is shifted as ν increases above unity, as seen in Fig. II.2.

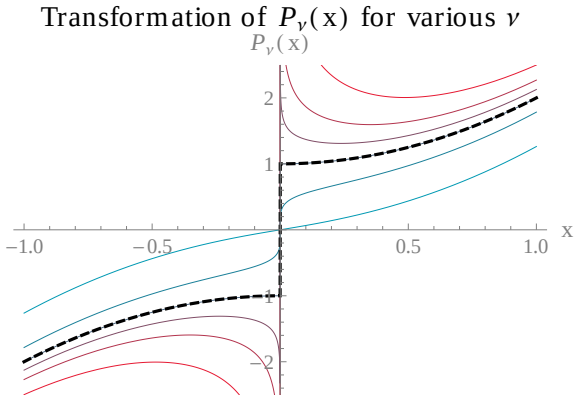

Figure II.1: The behavior of $\Delta_{\mathcal{R}}$, continued into $\mathbb{R}$ to emphasize behavior. The dashed black line corresponds to the de Sitter solution, with $\nu = 1$. For $\nu > 1$, the continued function is discontinuous at the origin and the spectrum of perturbations is redshifted. For $\nu < 1$, the function is continuous, but the spectrum is blueshifted.

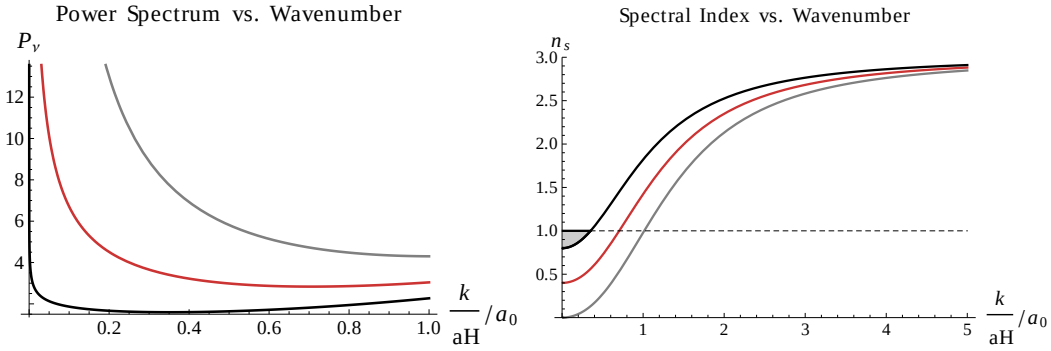

Figure II.2: The power spectrum and spectral index for $\nu = 1.5, 1.3$ and 1.1. In both cases k/aH is normalized for clarity. Note that for observationally relevant scales, inflation pushes the $k \ll 1$, making n_s slightly less than one a self-consistent prediction. This is illustrated in the shaded region for $\nu = 1.1$.

CHAPTER III

INTERLUDE ON THE STRING LANDSCAPE

III.1 A Vast Solution Space

The traditional definition of a quantum vacuum is the the lowest energy state of a system. For a quantum field theory, a simple example would be a zero-particle state. Systems which admit scalar fields have a more complex vacuum structure, although one typically searches for the global minimum of the scalar potential. This search may lead to straight forward interpretation. Among a set of not-necessarily degenerate local minima, a system may reside in a higher energy state before tunnelling into the true vacuum [58, 59]. Direct computation of these effects are rather delicate given the difference between Lagrangian and Hamiltonian path integrals [60].

Given the unsolved problem of quantum gravity, what is meant by a gravitational vacuum is less clear. This issue is further obfuscated by dynamic evolution of the observed universe. The classical vacuum is certainly one with maximal symmetry, typically Minkowski space. For constant, negative spacetime curvature, a quantum theory of gravity has been defined in terms of the conjectured AdS/CFT correspondence [61]. With the observation of late-time cosmic acceleration [62, 63], it is plausible that we exist in a matter-filled, de Sitter universe. The presence of matter breaks the de Sitter isometries of spacetime down to the FLRW metric, but following our notion of a particle vacuum above, one could define the gravitational vacuum today blithely with the de Sitter metric.

String theory is the dominant paradigm for studying the effects of quantum gravity, and the preceding observations are certain motivation to look for time-independent, de Sitter backgrounds. This is not easy. Time-independent string theory backgrounds which admit a geometric interpretation — *i.e.* those we are most equipped to handle — are ten-dimensional and supersymmetric. Kaluza-Klein [64] compactification to four dimensions is possible, although fraught with complications. These technical details can be subverted with the aid of supersymmetry, providing the added benefit of stability. Unfortunately, four-dimensional, de Sitter, $\mathcal{N} = 1$ supersymmetry does not exist [65].

Given our present understanding of string theory and the universe, a construction of the latter within the framework of the former appears to be necessarily complicated. For a clear and detailed discussion of why this should be — and for further reference on string vacua — see Ref. [7]. In what follows we discuss one particular scenario for realizing de Sitter vacua in string compactifications. It is conjectured to afford an extremely large quantity of plausible solutions, which allows us to approach some notion of a "generic" de Sitter compactification [66, 67].

III.2 Kachru-Kallosh-Linde-Trivedi Moduli Stabilization

In their seminal work, Kachru, Kallosh, Linde and Trivedi (KKLT) [68] drew from a large body of different results in string theory and quantum gravitational effects to stabilize all the moduli in IIB supergravity compactifications. Their final result was a meta-stable, four dimensional de Sitter vacuum whose lifetime to decay was consistent with cosmological observations. Much of the subsequent work in string phenomenology has been based on this construction.

In the KKLT approach, the complex structure moduli and axio-dilaton are assumed to be fixed by $G_3 \in H^{(2,1)}(X,\mathbb{Z}) \oplus H^{(0,3)}(X,\mathbb{Z})$ flux by means of the Gukov-Vafa-Witten superpotential [69],

$$W_0 = \int_X G_3 \wedge \Omega,$$

here Ω is the holomorphic three-form associated to Calabi-Yau manifold X. SUSY solutions require that G belong to $H^{(2,1)}(X,\mathbb{Z})$, so the fluxes need to be tuned such that the $H^{(3,0)}$ contribution is small. This has the added benefit of stabilizing the volume modulus at large VEVs large enough suppress α' terms and otherwise maintain the supergravity approximation.

The superpotential is fleshed out by nonperturbative corrections which may either come from D3 instantons or strong gauge dynamics on D7 branes wrapping four-cycles in X. In either case, the resulting superpotential is

$$W = W_0 + \sum_i A_i e^{-a_i \sigma},$$

where the Gukov-Vafa-Witten contributions W_0 is effectively a small constant. The exponent a_i is either 2π or $2\pi/N$, where N is the rank of the D7 worldvolume gauge theory undergoing gaugino condensation. In the presence of additional magnetic flux, such a term may be generalized to

$$e^{-a_i \sigma} \to e^{-a_i \sigma + f}, \tag{III.1}$$

where f is a phenomenological parameter $\mathcal{O}(100)$ which represents the extra size supported by the energy density of additional flux threading the four-cycle populated with D7-branes.

These nonperturbative contributions to the superpotential is crucial, as a shift-symmetry in the volume modulus σ prevents perturbative contributions to the superpotential. For the volume superfield T,

$$\sigma = -i(T - \overline{T}).$$

Note that we have implicitly assumed that the axionic part of T, $C_T = T + \overline{T}$ is stabilized at zero.

All that remains to be stabilized is the Kähler moduli. In KKLT models, it is typically assumed there is but a single such modulus, although generalizations have been studied. The effective Kähler potential for a single-field model is of no-scale form,

$$K = -3 \log\left[-i(T - \overline{T})\right],$$

which leads to the scalar potential,

$$\mathcal{V} = e^{K}\left(K^{T\overline{T}}D_{T}W\overline{D_{T}W} - 3|W|^{2}\right).$$

Here the Kähler covariant derivative is $D_{T}W = \partial_{T}W + K_{T}W$ and the Kähler metric in field space is

$$K_{T\overline{T}} = \partial_{T}\partial_{\overline{T}}K,$$

to which $K^{T\overline{T}}$ is the inverse.

Finally, SUSY is broken explicitly by the addition of $\overline{D3}$ branes [70] — D3-branes which preserve a different set of the thirty-two, ten-dimensional supersymmetry generators. In the presence of imaginary-self dual 3-form fluxes, their contribution can be made small by warping of the type found in "throat" geometries constructed by Klebanov and Strassler [71], and thereby under parametric control. A phenomenological parametrization of the scalar potential is then

$$\boxed{\mathcal{V} = e^{K}\left(K^{T\overline{T}}D_{T}W\overline{D_{T}W} - 3|W|^{2}\right) + \frac{8c}{\sigma^{3}}.} \tag{III.2}$$

III.3 The Kallosh-Linde Problem

III.3.1 Scales of SUSY Breaking and Inflation

The KKLT paradigm of lifting the vacuum energy to de Sitter space with an explicit SUSY breaking term in the scalar potential manifestly introduces a new energy scale into the system. For the simplest models, this uplifting is used implicitly to dial in an inflection point for the scalar potential. In such a scheme, the scales of inflation and SUSY breaking are related.

As pointed out in a paper by Kallosh and Linde [72], this creates a tension between high scale inflation and weak scale SUSY. For inflation to exist near the Planck scale, as one might naïvely expect, the scale of introduced by uplifting must be substantial. To maintain the conventional phenomenology favored by weak-scale SUSY breaking, such an uplifting seems to exclude the possibility of an inflection point.

Kallosh and Linde effectively argued that minimal KKLT scenarios could not work, and proposed that at least some extension was required. They demonstrated that this problem could be solved in Racetrack Inflation [73], where a Minkowski vacuum and high scale inflection point could be generated by the interplay of nonperturbative terms in the superpotential.

III.3.2 A Simple Realization

Of course, this phenomena can be anticipated on physical grounds. In simple models, the uplifting term is the relevant scale for both inflation and SUSY breaking. To separate these effects, one must introduce a new scale into the problem. Kallosh and Linde effectively managed this with

two nonperturbative terms. As we shall see, this is not enough. For a hierarchy between inflation and SUSY breaking requires a hierarchy in couplings.

Indeed, the fundamental mathematics which underpins these effects can be modelled by a simple quintic polynomial,

$$\mathcal{V} = \frac{1}{5}x^5 + \frac{1}{3}ax^3 + \frac{1}{2}bx^2 + cx + \text{constant}, \tag{III.3}$$

where a (Tschirnhaus) shift in x is used to eliminate the quartic term. To demonstrate the effect of the Kallosh-Linde problem, let us fix $a = -1$ and examine the behavior of $\mathcal{V}$ for various b and c. We will indeed fine that the set of physically viable inflection points is indeed limited.

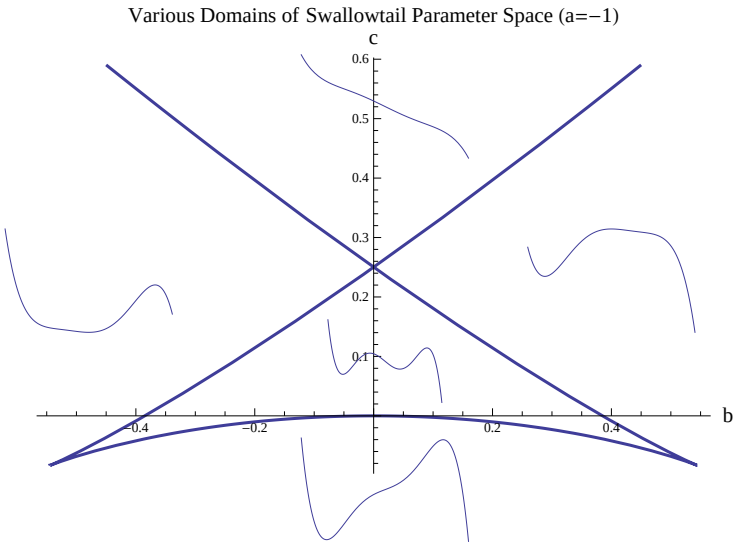

Figure III.1: Plot of the parameter space of the potential from (III.3). The behavior of $\mathcal{V}$ in different regions of parameter space is superimposed for reference.

The purple, piecewise smooth curve in Fig. III.1 represents the set of b and c which allow for simultaneous solutions to the equations

$$\frac{dV}{dx} = 0, \quad \frac{d^2V}{dx^2} = 0.$$

In particular, each point on the curve corresponds to a potential with an inflection point. This curve divides the parameter space into three domains. The domain inside the triangle has two local minima. The Domain below the diverging "wings", but outside the triangle have a single minimum. The upper domain has none. Another way to interpret the curve is the set of marginally stable configurations of $\mathcal{V}$ which interpolate between these domains.

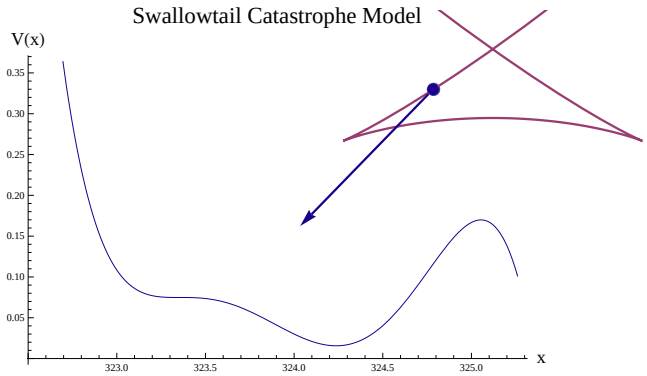

Figure III.2: Plot of a IIB "Racetrack" potential in blue. It has the same structural behavior as $\mathcal{V}$ from (III.3). The purple feature is the same parameter space from Fig. III.1. The specific point in this parameter space is highlighted for rerefence.

To maintain the phenomenologically desirable combination of an inflection point above a local minimum — with a barrier to a runaway — the potential must take values on the left hand side of the triangular region only. That we only have access to a single segment of a curve of possible inflection points is a precise restatement of the observation of Kallosh and Linde. For example, if one chooses a point above the apex of the triangular region, the physical vacuum and its barrier to runaway vanish. As critical points of $\mathcal{V}$, they collide at the apex and become complex-valued. This is illustrated in Fig. III.2.

We have an additional degree of freedom at our disposal. The size of the triangle region scales with $|a|$ in (III.3). To separate the scales of inflation and SUSY breaking — in this case the difference in $\mathcal{V}$ between the inflection point and the local minimum — one must increase a. This amounts to separating these two critical points in field space. In other words, the hierarchy of scales is generated by a hierarchy in critical point VEVs.

This discussion would be a cute toy model if not for some powerful theorems of V.I. Arnold [16] regarding the normal forms of smooth functions. As we discuss in the next chapter, the relationship between the quintic polynomial (III.3) and the supergravity scalar potential (III.2) is no coincidence. For a smooth, real function with three parameter to vary, such behavior is completely generic. We use this fact as a starting point for our analysis: to classify and study the set of all generic inflection point inflationary models.

III.4 What We Talk About When We Talk About the Landscape

The Landscape of String vacua is most often discussed in terms of local minima to an effective potential arising from a Kaluza-Klein compactification.

III.4.1 A Pointillist Solution Space

In the early days of string theory, conventional wisdom held that there as a single background solution — a unique vacuum — which would give rise to all the observed physics. Consistency relations required the vanishing of the four-dimensional cosmological constant, which was heralded as a success. Then in 1998 the High-z Supernovae Search team announced evidence for late-time, cosmic acceleration [62]. This finding was followed up shortly by the release of similar results by The Supernova Cosmology Project [63]. The existence of a small, but non-vanishing cosmological constant — or approximation thereof — is an extreme fine-tuning problem and a major open problem.

Meanwhile, the study of moduli stabilization in string theory had revealed an extremely large, but discrete space of supersymmetric solutions using magnetic flux background. The discrete nature of the solution space comes from quantization conditions on the fluxes when integrated over compact manifolds, not unlike Dirac's quantization condition in his study of magnetic charges.

Calabi-Yau 3-folds are often characterized by the dimensions of two Dolbeault cohomology groups: $h_{1,2} = \dim H^{(2,1)}$ and $h_{1,1} = \dim H^{(1,1)}$. Compactness, Ricci flatness, Complexity and Hodge and Poincaré duality constrain the rest of cohomology groups to depend on these two numbers. In general, these numbers — and the number of associated internal cycles — can be in the hundreds. In string theory, different types of magnetic flux can thread these various cycles in configurations numbered by integers as per the quantization conditions. Counting the vast number of possible models based on such a set up has lead to numbers on the order of $\mathcal{O}(10^{500})$ or higher.

The conjectured **Landscape** of flux vacua starts with the existence of a similarly enormous set of anti-de Sitter vacua. These can be any number of the well motivated examples in F-theory [74, 75], but perhaps also orientifold compactifications [76, 77, 78]. Despite some recent investigations [79, 80], the details of uplifting the vacuum energy to de Sitter space is not well understood, and there is compelling evidence that it may be a flawed concept [81]. Allowing for uplifting and meta-stable vacua leads one to the study of Eternal Inflation, which is reviewed in this context in [82] and the references therein.

Our philosophy on the uplifting issue is semi-ambivalent: while we do need positive vacuum energy, we do not need it to come from a consistent string compactification of a particular type. Our dealings with the landscapes is predicated on its numerosity. The approach we advocate is that inflation — whatever drives it — can be used as a tool to coarse grain over such a large solution space.

Nevertheless, given the phenomenological success of Weinberg's anthropic explanation of the cosmological constant [33] a few comments are in order.

The conjectured **landscape of string theory vacua** brings together two ideas. The first is the discretuum of (also conjectured) phenomenologically viable meta-stable flux vacua. The second

is the possibility of integrating out all the six-dimensional, stringy physics into an effective, four dimensional scalar potential. Perhaps echoing the Reid conjecture[1], the conventional wisdom surrounding the landscape seems to suggest that each of the nearly infinite, discrete possibilities may correspond to a different local minimum of the effect potential. With a huge ensemble of possible states, one can then invoke the Weinberg argument [33] to postdict the existence of an incredibly small cosmological constant from string theory. The main issue [81] with this assumption is whether or not different somehow-deformed Calabi-Yau vacua can be considered different vacua of the theory, *viz.* the Coleman-de Luccia transitions [85].

In any case, given an intractably large landscape of *candidate* vacuum solutions to string theory, our goal is to paint over it with different classes of inflationary models. Aside from giving a handle to deal with such an potentially unruly ensemble, it also takes a first step towards thinking about vacuum selection.

III.4.2 Our Takeaway

The main insight we take from these ideas is that a large solution set of possible universe should be taken seriously. Since $10^{500} - 10^{1500}$ amounts to infinity in phenomenological terms, it is fair to look for a "generic universe" and compare ours to it. The required sixty or so e-foldings of inflation suggests some sort of fine tuning. While the main goal is uncover new physics responsible for such a tuning, we must first attempt to make the notions of generic and tuning precise.

The analysis put forth in this work is largely based on semi-classical analysis. Given our assumptions, spelled out below, we conclude that inflation is generically absent. The number of e-foldings amounts to a tuning between couplings in the scalar potential to bring about inflection point inflation. This result hinges on the fixed point dynamics enjoyed by inflection points. We essentially expand the minisuperspace analysis to include all possible couplings in the scalar potential.

Without detailed knowledge of the ultraviolet physics, it is impossible to determine the correct measure on phase space. Regardless, our analysis demonstrates that the choice of scalar potential and inflection point inflation both play important roles in any statistical analysis — and are sometimes deeply related.

[1]The mathematician Miles Reid conjectured that moduli spaces of topologically distinct Calabi-Yau 3-folds may be connected [83] by means of conifold transitions [84].

CHAPTER IV

STRUCTURAL CLASSES FOR INFLECTION POINT INFLATION

In this chapter we introduce a classification of inflection point models based on the stability properties of the scalar potential. By restricting our focus to critical points, this classification affords a coarse-grainning over possible embeddings of inflection point inflation. This analysis is based on the work in Ref. [34].

IV.1 Motivation for a Classification

Doubly degenerate critical points of a function can always be modelled by cubic functions. This simple fact means that results like the number of e-foldings (II.19) are universal amongst inflection point models. Such universality descends from universal prescriptions for the local expansion of smooth functions.

These ideas were first studied as surface singularities by Patrick du Val[86] in the Thirties. Applications of these ideas to more general situations were studied *en masse* by René Thom [87]. Thom's Catastrophe Theory studied how critical points of real functions degenerate. Here Thom and others emphasized how the changes to the stability structure of a physical system could be modelled by catastrophe's like the Swallowtail studied above. This classification scheme was considerably extended and made rigorous by V.I. Arnold [16].

Our analysis centers on critical points of the scalar potential. We will be interested in their behavior as the couplings in the potential are varied. As we discuss below, the maximum number of local extrema accessible by variation of the couplings determines the stability structure of the potential. This sets up our arena. Our game is then to find all possible ways two critical points can degenerate — all possible models of inflection point inflation within said arena. We then extract whatever information we can from these structures alone.

We have two goals in this analysis. First, we aim to facilitate a better understanding of how inflation embeds into larger theories like string theory and particle physics. Second, we look for observational signatures distinct to each structural class. Later chapters in this dissertation spell out progress on both these fronts. First, however, we must develop the relevant technology.

IV.2 Arnold's Classification of Normal Forms of Smooth Functions

In this and what follows, we make extensive use of the qualifier **generic**. Mathematically, we take generic to mean "all but a set of measure zero". For points in Euclidean space, this is a sensible notion. For a particular function among a set of smooth functions it may be less so. A smooth function is at least locally diffeomorphic to a finite polynomial whose coefficients are generic as above. We may, however, assume the existence of a discrete symmetry, like the $\mathbb{Z}_3$-invariant

potentials in Chapter V. Hence, one may consider polynomials in ϕ^3. Generic then has a natural meaning modulo that symmetry.

Physically, we mean to avoid hidden conspiracies or fine-tuning. Without a guiding notion of what string theory, particle physics, or whatever model bests describes the earliest moments of the universe, we take take a philosophy of non-exceptionalism, not unlike the modern approach to cosmology. While all models of inflation seem to require some fine-tuning, we prefer to keep the tuning explicit and therefore under control.

Given a generic, smooth function $\mathcal{V}$ of finitely many variables and control parameters which has no more than two vanishing eigenvalues of the Hessian, Arnold proved that at a critical point, a diffeomorphism exists which can bring to one of the following generic forms or "germs":

$$\mathcal{V}_{A_k} = \frac{1}{k+1}x^{k+1} + Q^2, \tag{IV.1}$$

$$\mathcal{V}_{D_k} = \frac{1}{k-1}x^{k-1} + xy^2 + Q^2, \tag{IV.2}$$

$$\mathcal{V}_{E_6} = y^3 + x^4 + Q^2, \tag{IV.3}$$

$$\mathcal{V}_{E_7} = y^3 + yx^4 + Q^2, \tag{IV.4}$$

$$\mathcal{V}_{E_8} = y^3 + x^5 + Q^2. \tag{IV.5}$$

Here Q^2 represents a standard quadratic form, perhaps in the other variables. There is a "splitting" lemma which states than there is always a smooth change of variable which allows one to locally split into non-Morse variables and the standard Morse part. Recall that a Morse function is one whose critical points are (Hausdorff) separated.

Arnold's proof went further: if the space of control parameters is less than six dimensional, $\mathcal{V}$ must take one of these forms; a third eigenvalue of the Hessian cannot be made to vanish. Higher singularity germs all contain moduli: a diffeomorphism of the manifold near the critical point will bring you back to the same family of germs, perhaps with different values for the moduli. The one-moduli families of germs were studied extensively by Arnold, and can be found in [16].

An important extension of this classification is that the germs are deformed in a universal[1] way.

[1] Arnold called such universal deformations "versal" to emphasize the fact that they are generic. In general there are "versal", "mini-versal" and "universal" deformations. See [16] for details.

$$\delta\mathcal{V}_{A_k} = \sum_{n=1}^{k-1} \frac{a_n}{n} x^n, \tag{IV.6}$$

$$\delta\mathcal{V}_{D_k} = \sum_{n=1}^{k-2} \frac{a_n}{n} x^n + cy, \tag{IV.7}$$

$$\delta\mathcal{V}_{E_6} = c_3 x^2 y + c_2 xy + c_1 y + a_2 x^2 + a_1 x, \tag{IV.8}$$

$$\delta\mathcal{V}_{E_7} = c_2 xy + c_1 y + \sum_{n=1}^{4} \frac{a_n}{n} x^n, \tag{IV.9}$$

$$\delta\mathcal{V}_{E_8} = y \sum_{n=0}^{3} \frac{c_n}{n} x^n + \sum_{n=1}^{3} \frac{a_n}{n} x^n. \tag{IV.10}$$

Note that not all possible terms have been written. For example, x^k is absent from $\delta\mathcal{V}_{A_k}$ and xy is absent from $\delta\mathcal{V}_{D_k}$. These can be removed by a shift, changing the overall constant term in $\mathcal{V}$. This term is accounted for in the quadratic form Q^2. Since we are interested in the functional form of $\mathcal{V}$, we can leave such terms implicit. Physically, the constant term is related to the cosmological constant. This is a different matter, and in this work we assume that this issue is unrelated.

IV.3 A-type

IV.3.1 The Fold

The prototype for structural stability comes with the A_2 Model, known first by Thom as the "fold". Here

$$\mathcal{V}_{A_2} = \frac{1}{3} x^3 + ax + \text{constant}. \tag{IV.11}$$

For negative a, $\mathcal{V}_{A_2}$ has two local extrema. For positive a there are none. A degenerate critical point exists if and only if a vanishes. When $a \ll 1$, this behavior is universal to a nearly degenerate critical point of any smooth function. This behavior is shown in Fig. IV.1.

IV.3.2 The Cusp

The A_3 potential, known to Thom as the "cusp", yields more complete model.

$$\mathcal{V}_{A_3} = \frac{1}{4} x^4 + \frac{1}{2} ax^2 + bx + \text{constant}.$$

Here there are at most three critical points. For positive a, $\mathcal{V}_{A_3}$ has only one minimum; two critical points are complex-valued. To obtain three local extrema from one by varying the (real) parameters a and b , $\mathcal{V}_{A_3}$ must pass through a degenerate critical point. This amounts to the condition,

$$\left(\frac{a}{3}\right)^3 + \left(\frac{b}{2}\right)^2 = 0. \tag{IV.12}$$

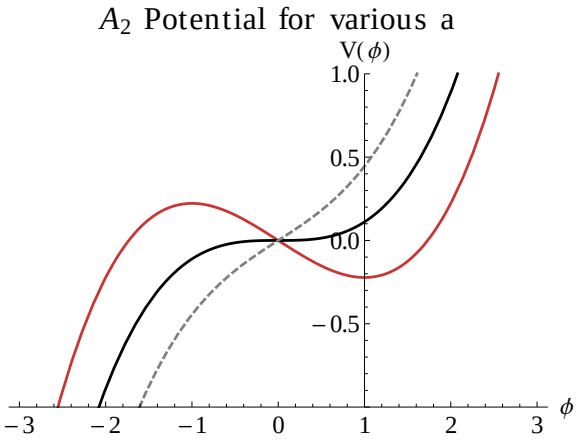

Figure IV.1: The Fold potential from (IV.11). For $\mathfrak{a} = -1$, there is a local minimum. $\mathcal{V}_{A_2}$ becomes metastable as $\mathfrak{a}$ vanishes. The dotted curve corresponds to $\mathfrak{a} = 1$, where the critical points have become imaginary.

Eqn. (IV.12) represents a co-dimension one subvariety of parameter space. Call this space $\mathcal{M}_{A_3}$ This is represented by the bold curve in Fig. IV.2. The cusp feature near the origin gives rise to Thom's name for this singularity germ. $\mathcal{M}_{A_3}$ serves as domain wall in parameter space, dividing the one-minimum family of potential from the two-minimum family by a those with a degenerate critical point.

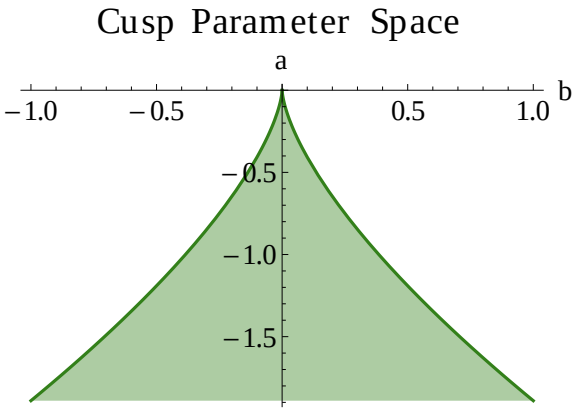

Figure IV.2: The cusp parameter space cut by the piece-wise smooth curve $\mathcal{M}_{A_3}$. The shaded region has two local minima, while the unshaded region has only one. $\mathcal{M}_{A_3}$ comprises the subset of points for which $\mathcal{V}_{A_3}$ has a degenerate critical point.

Let α parametrize this curve so that α vanishes at the origin of parameter space. Then by (IV.12), $\mathfrak{a} = -3\alpha^2$ and $\mathfrak{b} = 2\alpha^3$. Then $\alpha \in \mathbb{R}$ defines a one-parameter family of inflection point models based on $\mathcal{V}_{A_3}$. The constant in $\mathcal{V}_{A_3}$ can be chosen to that the energy density at the local minimum

vanishes. Then,

$$\mathcal{V}_{\text{cusp}} = \frac{1}{4}x^4 + \alpha x^3 + \frac{27}{4}\alpha^4. \tag{IV.13}$$

Here we have shifted x to $x + \alpha$ so that x vanishes at the degenerate critical point. The global minimum occurs at $x = -3\alpha$. Notice that the energy scale of inflection point inflation scales by α^4, as shown in Fig. IV.3.

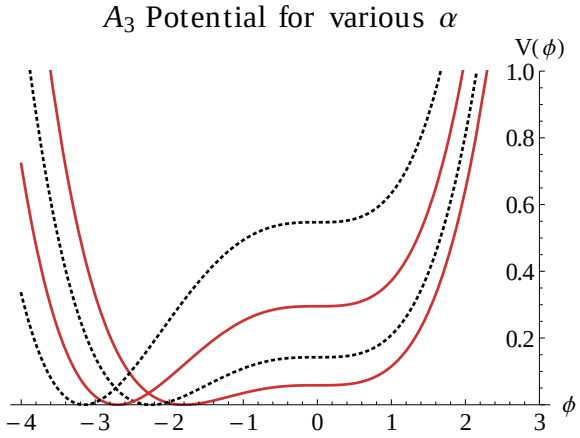

Figure IV.3: The cusp potential from (IV.13) for various α. Notice that as the seperation between the inflection point and the local minimum increases, so too does that value of the potential.

As with the fold, $\mathcal{V}_{A_3}$ is universal for small α. Since inflation requires a non-vanishing vacuum energy, we would expect α to be finite and (IV.13) to only be a qualitative description of the true potential. While the "critical" scaling of the energy density during inflation, α^4 will certainly change as α grows large, the parametric relationship between the seperation of scales and the seperation of critical points should remain.

As with the fold, the cusp can be deformed away from a degenerate critical point by moving off the subvariety $\mathcal{V}_{A_3}$. Near the degenerate critical point — *i.e.* near $x = 0$ — the physics is well modelled by the fold potential. Put differently, since a large amount of inflation is required physically, the deviation from locally cubic behavior can be parametrized by the relevant operator x with a small coupling, $\lambda \ll \alpha^3$.

The deformed potential is then

$$\mathcal{V}_{\text{cusp}} = \frac{1}{4}x^4 + \alpha x^3 + \lambda x + \frac{27}{4}\alpha^4, \tag{IV.14}$$

and by (II.19), the number of e-foldings of inflection point inflation is approximately,

$$N_e \approx \frac{\pi}{2\sqrt{3\alpha\lambda}}.$$

This behavior is demonstrated in Fig. IV.4.

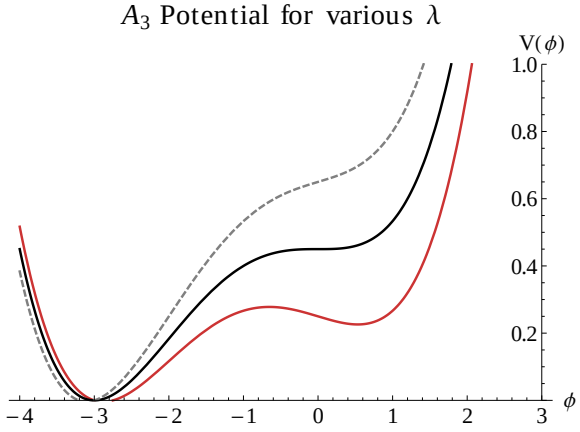

Figure IV.4: The deformed cusp potential from (IV.14). The same sign dependence of the tadpole coupling, λ appears as with the fold.

The point is important so we stress it again. The A_3 germ unfolds by deformation to a one parameter family of A_2 germs. In the language of spontaneous symmetry breaking, α is the order parameter for the $SU(4) \to SU(3)$ breaking, and all the physics induced by this breaking depends the value of α.

Note that most simple model of hybrid inflation [19] also fall into this category, although they are two field models. The A_3 germ corresponds to the critical value of the inflaton where the so-called waterfall phase transition takes place.

IV.3.3 The Swallowtail

To drive home these ideas and make contact with string compactifications, we consider finally the A_4 model known to Thom as the "swallowtail". Here the potential is

$$\mathcal{V}_{A_4} = \frac{1}{5}x^5 + \frac{1}{3}ax^3 + \frac{1}{2}bx^2 + cx + \text{constant}. \tag{IV.15}$$

There are four critical points and three control parameters. Therefore the codimension-one subvariety of points leading to degenerate critical points of $\mathcal{V}_{A_4}$ will be two dimensional. This space, $\mathcal{M}_{A_4}$, is parametrized by two parameters α and β. To determine this parametrization, let

$$\frac{\partial \mathcal{V}_{A_4}}{\partial x} = (x-\alpha)^2(x-\beta)(x-\gamma).$$

The critical point γ will be fixed by same shift in x used to cancel quartic term in (IV.15). Now,

$$(x-\alpha)^2(x-\beta)(x-\gamma) = x^4 + ax^2 + bx + c,$$

so by matching coefficients of x, we find,

$$\begin{aligned} 2\alpha+\beta+\gamma &= 0, && \text{(IV.16)}\\ \alpha^2+\alpha(\beta+\gamma)+\beta\gamma &= a, && \text{(IV.17)}\\ \alpha^2(\beta+\gamma)+2\beta\gamma\alpha &= -b, && \text{(IV.18)}\\ \alpha^2\beta\gamma &= c. && \text{(IV.19)} \end{aligned}$$

Eliminating γ, we find

$$\begin{aligned} a &= -2\alpha^2-(\alpha+\beta)^2, && \text{(IV.20)}\\ b &= 2\alpha(\alpha+\beta)^2, && \text{(IV.21)}\\ c &= -\alpha^2\beta(\alpha+\beta). && \text{(IV.22)} \end{aligned}$$

Note that these equations include scaling relationships,

$$\frac{b}{a^{3/2}} = -4\alpha^2+2\alpha, \quad \frac{c}{a^2} = 3\alpha^4-\alpha^2, \qquad \text{(IV.23)}$$

which allows us to examine a cross-section of $\mathcal{M}_{A_4}$ in $\mathbb{R}^3$. Effectively, we need only consider the cases where $a = \pm 1$ or 0, the rest are related by scaling. This simplification facilitates the discussion of A_4 phenomena.

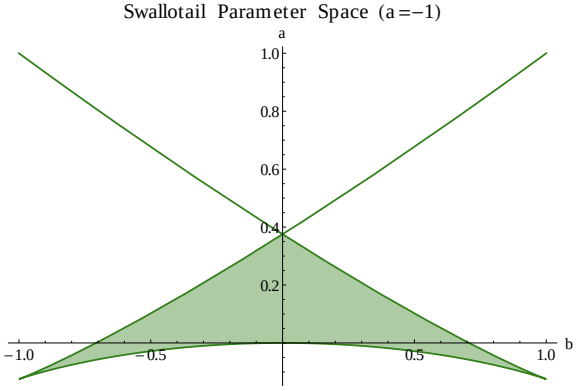

Figure IV.5: A cross section of the A_4 parameter space, with $a = -1$. As with Fig. IV.2, the piecewise smooth curve represents the subset of couplings for which $\mathcal{V}_{A_4}$ has a degenerate critical point. The shaded region corresponds to a $\mathcal{V}$ two local minima, the bottom connected component has one, and the top has none.

Eqn. (IV.23) represents a family of curves in the space of couplings in which $\mathcal{V}$ has a degenerate critical point. For positive a, this curve divides a single metastable state from a runaway, not unlike the fold singularity. Indeed, it can be locally approximated as such, with the strength

of the cubic coupling depending on α and β. Since we are typically interested in stabilized[2] scalar fields, this is not a case of physical interest. For vanishing $\mathfrak{a}$ this holds true, except in the vicinity of vanishing α, where a local quartic model is appropriate. Finally, negative $\mathfrak{a}$ allows for inflection point inflation and a meta-stable vacuum. Potentials with both features exist for the left half of the triangular region shown in Fig IV.5. The right half of the triangle involves inflection point inflation towards a runaway. At the midpoint of the base the barrier degenerates to form an inverted quartic, while at the apex the local minimum degenerates to form a second inflection point. This finite region (relative to β) of physically relevant models explains quantitatively the Kallosh-Linde phenomena. This is illustrated in terms of the potential on the left side of Fig. IV.6. The right side compliments this by showing a deformation away from the triangular boundry illustrated in Fig. IV.5. The hierarchy of the scales between inflation and SUSY breaking is explained with simple algebra; it merely requires a hierarchy between the values of α and β.

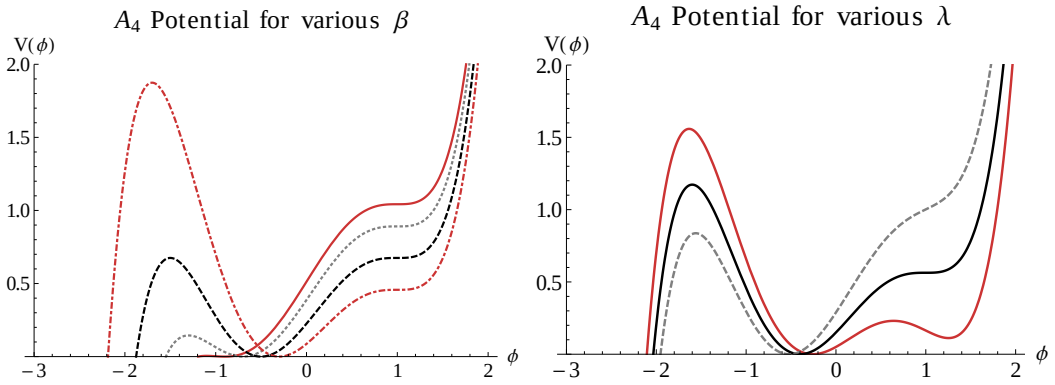

Figure IV.6: The swallowtail family of potentials under the variation of various couplings. On the left, note the strong dependence of the barrier height on the coupling β, compared with the tadpole coupling λ on the right.

IV.4 D-type

IV.4.1 On Multiple Fields

When multiple scalar fields have a mass lighter than the Hubble scale during inflation, the dynamics are substantially enriched. The set of real critical points now include saddle points, which can degenerate to form a variety of potential energy landscapes for the inflaton to roll through.

The perturbations are also effected. If the mass of a spectator scalar field φ is larger than the Hubble scale, that is $V_{\varphi\varphi} \gg H^2$, the perturbations are strongly suppressed. From (II.32), we find

[2]Quintessence models of Dark Energy utilize a slowly-rolling scalar field to drive accelerated expansion, not unlike inflation. Such considerations may be relevant here, although the process of reheating and our cosmic history obfuscate any relation between the inflaton and a possible quintessence field. For a short review of Quintessence, see Ref. [88].

that the modes can be solved in terms of spherical Hankel functions $\delta\varphi \sim x h_\nu^i(x)$, whose index in this limit becomes

$$\nu \to -i\frac{V_{\varphi\varphi}}{H^2},$$

which implies that $|\delta\varphi| \to 0$.

Once φ becomes light two things can happen. First, the spectator perturbations can also become important. These are **isocurvature perturbations** because they disturb the mixing of matter, not its density. They seed **entropy perturbations**, not curvature perturbations. Second, the naïve inflaton and ϕ can mix. Not only does this open parameter space, but they mixing can change over the course of inflation. In such a case the would-be entropy perturbations can be transmuted into curvature perturbations. These nonlinear effects can have a sizable impact on the statistical distribution of observed thermal fluctuations in the CMB. Such effects have not been observed [9], giving an important constraint on such models.

As with single field degenerate critical points, there are only so many ways a function may exhibit two extremely light, massless fields in a generic fashion. For an additional field which interacts very weakly with itself, we find the D-type models. Stronger self-interacting fields are discussed in the next section.

IV.4.2 D-type Generalities

The D_k-type potential is

$$\mathcal{V}_{D_k}(x,y) = \frac{x^{k-1}}{k-1} + xy^2 + \sum_{n=1}^{k-2} a_n x^n + cy + \text{constant}. \tag{IV.24}$$

While we have little use for such an *a priori* distinction, for even k, one often distinguishes between $D_{\pm 2k}$ by the germs,

$$\mathcal{V}_{D_k} = x^{2k-1} \pm xy^2.$$

In this language, the D_{-2n} germs are known as a monkey saddles, a moniker which can be visualized in Fig. IV.8. These should be contrasted to the D_{+2n} cases, which behave rather differently. The case of D_4 is illustrated in Fig. IV.9. The D_{2n+1} germs behave as a mixture of the two, as seen for the specific case of Fig. IV.7.

We now analyze the general possibility of inflection point inflation in D-type models. Starting from (IV.24), and defining,

$$V(x) = \mathcal{V}_{D_k}(x,0),$$

the set of critical points solve

$$y^2 = -V_x, \tag{IV.25}$$

$$y = -\frac{c}{2x}. \tag{IV.26}$$

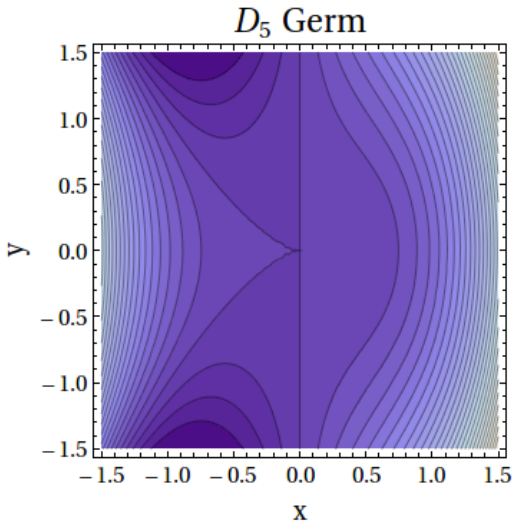

Figure IV.7: The D_5 model scalar potential plotted vs. field space on the left, and as contours in field space on the right. Note the concave approach towards a degenerate critical point at the center with two runaway directions to the left.

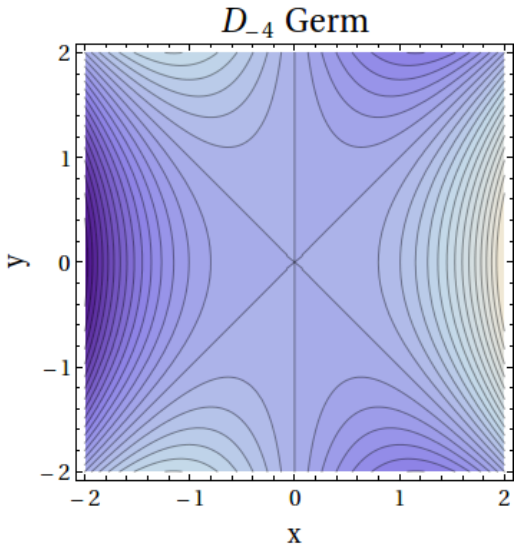

Figure IV.8: The D_{-4} model scalar potential plotted vs. field space on the left, and as contours in field space on the right. This is the archetype monkey saddle function. Note the convex approach towards a degenerate critical point at the center with two runaway directions to the left.

The Hessian matrix associated to $\mathcal{V}_{D_k}$ is

$$\mathfrak{H} = \begin{pmatrix} V_{xx} & 2y, \\ 2y & 2x \end{pmatrix}. \tag{IV.27}$$

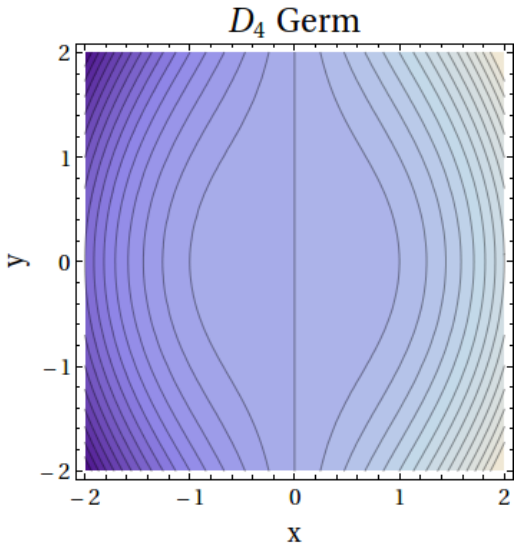

Figure IV.9: The D_4 model scalar potential plotted vs. field space on the left, and as contours in field space on the right. Note the concave approach towards a degenerate critical point at the center with single, convex runaway to the left.

The condition for a degenerate critical point is then the vanishing of $\det \mathfrak{H}$:

$$y^2 = \frac{xV_{xx}}{2} \tag{IV.28}$$

As seen in Figs. IV.10, IV.11 three curves (IV.25), (IV.26), (IV.28) generically intersect pairwise, at least in a connected subset of parameter space. Therefore, there is one fine tuning required to force a degenerate critical point, as with the A-type case. This is illustrated in the right side of Fig. IV.10. While a domain structure similar to the cusp and swallowtail certainly exist for D-type models, their dimensionality can rapidly get out of hand. Instead it is easier to work directly with these curves to plot out the various domains.

As Fig. IV.11 shows, (IV.25) is an elliptic curve. Such a curve can always be brought to Weierstrassß form,

$$y^2 = x^3 + Px + Q. \tag{IV.29}$$

For for negative P, the curve defined by (IV.29) is disconnected in the plane. For such a case, the curve passes between one-to-one and one-to-two as Q becomes positive. As the rank of the germ increases, so too do the possibilities. In any case, the study of critical points amount to the study of intersecting curves. For D-type germs, degenerate critical points require that the c parameter be tuned to bring the hyperbola of (IV.26) to the intersection point.

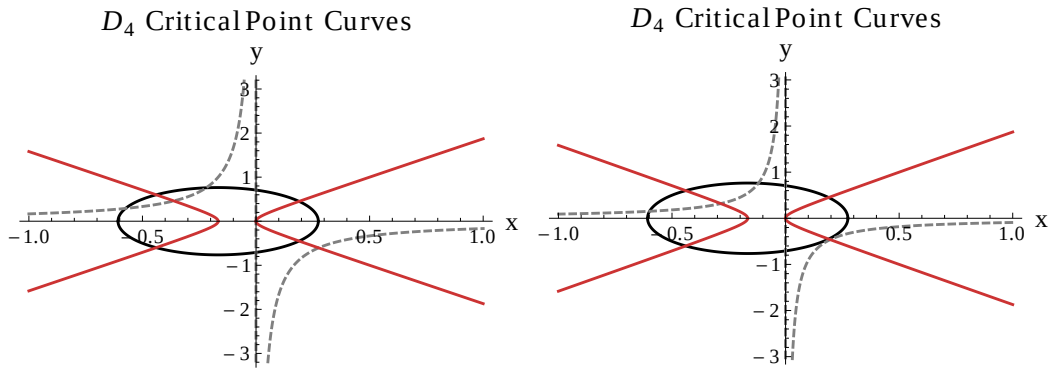

Figure IV.10: Curves in field space representing solutions to Eqns. (IV.25) (solid black), (IV.26) (dashed grey) and (IV.28) (solid red) for $k = 4$. The black and grey curves meet at critical points of $\mathcal{V}_{D_4}$. A generic configuration of parameters $(a_2, a_1, c) = (-1, -\frac{1}{2}, \frac{1}{3})$ is on the left. A set tuned for an approximate degenerate critical point $(a_2, a_1, c) = (-1, -\frac{1}{2}, \frac{1}{5.5})$ is on the right.

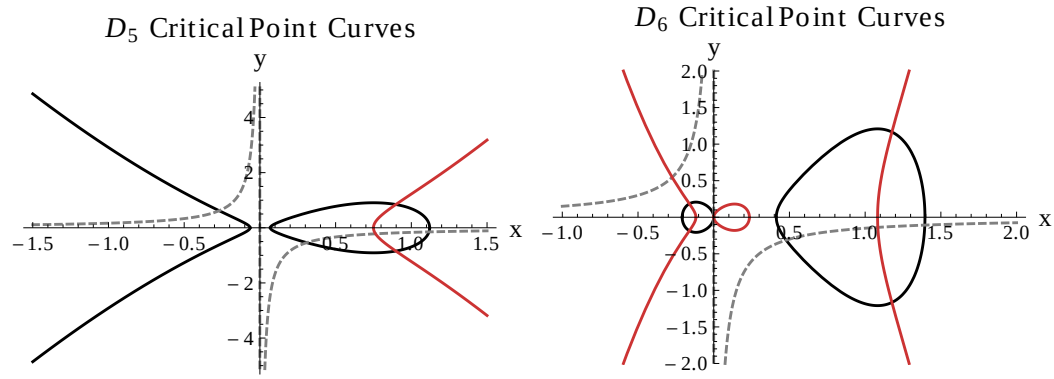

Figure IV.11: Curves in field space representing solutions to Eqns. (IV.25) (solid black), (IV.26) (dashed grey) and (IV.28) (solid red) for $k = 5$ on the left, and $k = 6$ on the right. The black and grey curves meet at critical points. These plots represent a generic configuration of parameters $(a_3, a_2, a_1, c) = (-\frac{3}{2}, 0, \frac{1}{50}, \frac{1}{3})$ on the left and $(a_4, a_3, a_2, a_1, c) = (-2, \frac{1}{3}, \frac{3}{5}, 0, \frac{3}{10})$ on the right.

IV.4.3 The D_5 *Model*

For concreteness, we consider the D_5 potential, whose germ is $\frac{1}{4}x^4 + xy^2$. This models has four deformation parameters, has a local extremum and allows us to understand breaking to the $D_{\pm 4}$ and A_3 models.

A one parameter deformation of the D_5 germ can be borrowed from (IV.13).

$$\mathcal{V} = \frac{1}{4}(x-\alpha)^4 + \alpha(x-\alpha)^3 + y^2(x-\alpha) + \alpha y^2 + \frac{27}{4}\alpha^4.$$

This effectively breaks D_5 down to A_3, as the eigenvalues of $\mathfrak{H}$ are zero and 2α. During inflation, y is pinned near zero with mass α. y also serves double duty as the tadpole for x, which needs to be small for inflection point inflation. This brings us to an important conclusion:

For large α, the D_5 potential admits a single field limit in x to the A_3 model.

For this deformation, x is the inflaton. If, in addition, one also requires a metastable vacuum at the end of inflation, further deformation is necessary. The addition of a mass term $\frac{1}{2}m^2\alpha$ does not affect the inflection point and stabilizes the vacuum so long as $m^2 > 3\alpha$. While this is not one of the canonical deformations listed in (IV.7), it can be obtained by a deformation followed by a suitable shift in x.

IV.5 E-type

E_k-type models complete the zoo of potentials that admit limits where two eigenvalues of the Hessian matrix vanish. For each $k = 6, 7, 8$, the germ is of cubic or higher order in both fields. This suggests use in models where self-interaction between the spectator are important.

$$\mathcal{V}_{E_6} = \frac{1}{3}y^3 + \frac{1}{4}x^4 + ax^2y + bxy + \frac{m_x^2}{2}x^2 + \lambda_x x + \lambda_y y + \text{constant}.$$

$$\frac{\partial \mathcal{V}_{E_6}}{\partial x} = x^3 + a2xy + by + m_x^2 x + \lambda_x. \tag{IV.30}$$

$$\frac{\partial \mathcal{V}_{E_6}}{\partial y} = y^2 + ax^2 + bx + \lambda_y. \tag{IV.31}$$

$$\mathfrak{H}_{E_6} = \begin{pmatrix} 4x^3 + 2axy + m_x^2 & 2ax + b \\ 2ax + b & 2y \end{pmatrix}.$$

Employing the same techniques as with the D-type case, we can understand how degenerate critical points arise. For positive or negative a, (IV.31) defines an ellipse or hyperbola in field space, respectively. (IV.30) yields,

$$(2ax + b)y = -\left(x^3 + m_x^2 + \lambda_x\right).$$

The Hessian condition amounts to,

$$(2ax + b)^2 = 2y\left(4x^3 + 2axy + m_x^2\right). \tag{IV.32}$$

In analogy with the D_5 case, the critical curves for a sample of E_6-class of potential are illustrated in Fig. IV.12.

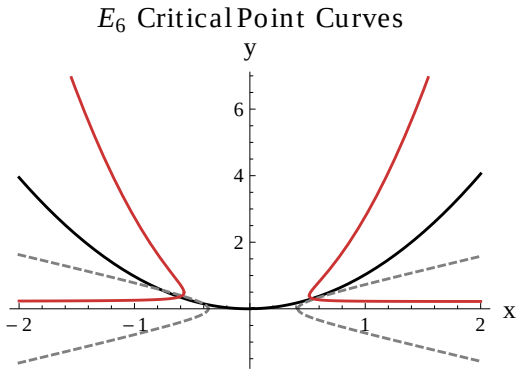

Figure IV.12: Curves in field space representing solutions to Eqns. (IV.30) (solid black), (IV.31) (dashed grey) and (IV.32) (solid red) for $k = 5$ on the left, and $k = 6$ on the right. The black and grey curves meet at critical points. These plots represent a generic configuration of parameters $(a, b, m_x^2, \lambda_x, \lambda_y) = (-2, \frac{1}{4}, \frac{1}{2}, 0, 0, 1)$.

IV.6 Of Normal Forms and the Simply Laced Lie Groups

We close this chapter with a discussion of the relationship between Arnold's classification scheme and the the Lie groups A_k, D_k and E_k. We explicitly construct a representation of A_k-type models from the characteristic polynomials of the adjoint representation of $SU(k+1)$, known by Cartan as A_k.

If the variables of a smooth function $\mathcal{V}$ parametrize a smooth manifold M, then $\mathcal{V}$ can be thought of as a function on M. Let Γ_M be the group of diffeomorphisms of M. The subgroup $G \subset \Gamma_M$ of diffeomorphisms which preserve the prescribed normal forms (IV.1)-(IV.5) of $\mathcal{V}$ are deeply related to the Weyl groups associated to the Lie algebras of A_k, D_K and E_K. The deformations (IV.6)-(IV.10) can likewise be thought of as symmetry breaking parameters, breaking the symmetry of the normal form down from one germ to another. Put differently, the germs nest within one another. The distance of critical points from the degenerate configuration — parameters like α and β above — can be interpreted as order parameters for this symmetry breaking. Roughly speaking, properties of the potential, like the height of barriers or the depth of minia, scale with these parameters. This scaling becomes exact near degeneracy. Since physical quantities depend on the features of the potential, they inherent these scalings automatically. In this sense Arnold's classification immediately generates a classification for inflection point inflation models.

Recall that the model for perturbed A_k-type potentials is

$$\mathcal{V}_{A_k} = \frac{1}{k+1}x^{k+1} + \sum_{n=1}^{k-1} \frac{a_n}{n}x^n.$$

By identifying $\mathcal{V}_{A_k}$ with the characteristic polynomial of some M_k in Adjoint representation of the Lie group A_k, we find that the a_n are related to specific sums of traces of products of M, as may be familiar from the study of the Cayley-Hamilton theorem. For example,

$$a_{k-2} = \frac{1}{2}\left[(\mathrm{tr}M)^2 - \mathrm{tr}M^2\right].$$

Now $\mathrm{tr}M$ is invariant under conjugation by any $g \in A_k$,

$$M \to gMg^\dagger.$$

Despite the fact that we focus on real $\mathcal{V}$, generally M is in the complexification of the Lie algebra of A_k. For one may always bring M to a linear combination of elements in the maximal torus of A_k,

$$M = \sum_{i=1}^{k} c_i\lambda_i,$$

then,

$$a_{k-2} = -\sum_{i=1}^{k} c_i^2,$$

and we are of course interested in both positive and negative a_n.

CHAPTER V

APPLICATIONS TO SUSY PARTICLE PHYSICS

This chapter looks investigates the phenomenological implications of inflation coupled to particle physics. We begin by describing the **minimal supersymmetric standard model** (MSSM), study inflation within the theory, and conclude with an brief example of applying the structural classification to particle phenomenology: the A_4 model in a KKLT-style compactifications.

V.1 The Minimal Supersymmetric Standard Model

V.1.1 The Standard Model of Particle Physics

The **standard model of particle physics** is a chiral gauge theory based on the group $SU(3) \times SU(2) \times U(1)$ with massless fermions and what recent observations suggest to be a single scalar field. Fermions in the fundamental representation of the $SU(3)$ (QCD) gauge group are called **quarks**. There are six named left-hand/right-hand pairs, ordered in increasing mass to be: up (U), down (D), strange (S), charm (C), bottom (B) and top (T). The left-handed quarks are also in the fundamental representation of $SU(2)$. They are paired up in doublets: (U,D), (C,S) and (T,B), where the $U(1)$ charges of (X,Y) are $+2/3$ and $-1/3$, respectively.

Those fermions which do not couple to the $SU(3)$ gauge bosons — those in the trivial representation — are called **leptons**. The left-handed leptons are also doublets under $SU(2)$: the electron pair (e, ν_e), the muon pair (μ, ν_μ) and the tau pair (τ, ν_τ). Right-handed e, μ and τ are known to exist owning to their Higgs-induced mass couplings, but neutrinos are assumed to be massless, so their left-handed partners are assumed to be absent.

Of course, neutrino masses have been observed via neutrino oscillations. But it is unclear what the nature of this mass is — *i.e.* whether or not it is Higgs induced.

As advertised, there is also a scalar field known as the **Higgs**. It breaks the $SU(3) \times SU(2) \times U(1)$ gauge symmetry down to $SU(3) \times U(1)$, with nontrivial mixing between the maximal torus of the electroweak — that is, non-QCD — sector.

V.1.2 The MSSM sparticles

To each aforementioned Standard Model particle, there is a superpartner or **sparticle**. This is, of course, the minimal scenario. The only major complication comes from the Higgs sector. Recall that the superpotential is holomorphic in chiral superfields. Therefore, giving mass to both the up and down quarks via superpotential terms like

$$\lambda_U U Q_1 H + \lambda_D D Q_1 H^\dagger,$$

while allowed by gauge invariance, would explicitly break SUSY. The simplest way out is to postulate two Higgs fields, say H_u and H_d which come as a negative-neutral and positive-neutral doublet, respectively. Thus superpotential terms like

$$\lambda_U U Q_1 H_u + \lambda_D D Q_1 H_d,$$

remain holomorphic and SUSY is preserved.

But there is more. SUSY ties weakly and electrically charged fermion to the Higgs. The **Adler-Bell-Jackiw anomaly** requires the sum of the electric charges of fermionic particles to vanish so that quantum effects do not spoil the electromagnetic gauge invariance. In some sense this explains the pairing of quarks (a doublet of whom has positive charge e) with leptons (whose doublet charge is $-e$). For this additional reason, an even number of Higgs doublets — with opposing total charges — are required by any SUSY extension of the Standard Model. The minimal choice is, of course, two.

If that were not enough, the **Witten anomaly** for $SU(2)$ also requires an even number of doublets.

One additional remark about phenomenological MSSM models. Generically, superpartners of Standard Model particles have the potential to introduce transitions not observed in nature. Strange quarks don't typically change into bottom or down quarks, despite having similar gauge quantum numbers. Similarly, higher dimensional couplings, even though suppressed by the scale of SUSY breaking, may induce proton decay at rates incompatible with observations. Happily, these problems can be mitigated by invoke an age-old tradition in particle physics, a new quantum number. Like strangeness or baryon number, R-parity may well be a reasonable symmetry of an effective MSSM. **R-parity** assigns a $+1$ to Standard Model particles, and a -1 to their superpartners. The overall action must be invariant under R-parity, and this simple requirement suppresses the phenomenologically dangerous couplings like those discussed above. As a bonus, it implies the existence of a stable superpartner, the **lightest supersymmetric particle** (LSP). Just like the electron cannot decay into neutrinos due to charge conservation, R-parity conservation forbids the LSP to decay. This leads to a natural dark matter candidate that predicts new interplay between particle physics and cosmology [89].

V.2 MSSM Inflation

In this section we study the embedding of inflection point inflation to supersymmetric quantum field theories. In particular, we show that the scale of inflation can arise solely from higher order terms in the superpotential. This greatly alleviates the fine-tuning that plagued applications to concrete models like MSSM-inflation. This work was originally reported in Ref. [35].

V.2.1 $\mathcal{D}$-flat Directions in the MSSM

There are a number of gauge invariant operators in the MSSM which do not pick up a classical potential. Such $\mathcal{D}$-flat directions were enumerated in Ref. [90]. In the MSSM they are cubic terms

in the superpotential, like

$$L_i L_j E_k, \quad \text{or} \quad U_i U_j D_k, \tag{V.1}$$

where all three flavor indices i, j, k are different.

Extending the MSSM to include right handed neutrinos increases the number of such flat directions, but will also induce quadratic terms, as such neutrinos are $SU(3) \times SU(2) \times U(1)$ singlets.

Such flat directions have a number of interesting implications for cosmology. For example, Affleck and Dine [91] demonstrated that they can be used for Baryogenesis which models the fortunate absence of antimatter in the universe. Other applications include inflationary cosmology. MSSM-inflation is an archetypal model for embedding inflation with supersymmetric particle physics.

These flat directions act as effective scalar degrees of freedom, and will be lifted by higher order terms.

$$W = \frac{\lambda}{3}\Phi^3.$$

V.2.2 Keeping it SUSY

There have been a number of attempts to incorporate inflation within the visible sector. Using a $\mathcal{D}$-flat direction such as (V.1) for the inflaton, inflation has been successfully embedded within the MSSM and some simple extensions thereof. Inflation occurs within the inflection point scenario, and the demands of weak scale SUSY fix the VEV of the inflaton orders of magnitude below M_P. Therefore, these class of models tends to be insensitive to their UV embedding.

Despite this traits, MSSM inflation has been subject to a technically unnatural fine tuning among the soft SUSY breaking couplings. This tuning can be softened by bringing the VEV closer to M_P, but the cost is a high scale of SUSY breaking. Such a scenario though plausible is not appealing for SUSY particle phenomenology.

In [35], we addressed the tuning problem directly by offering a general construction for inflection point inflationary models in supersymmtric field theories at sub-Planckian field VEVs. In particular, the SUSY preserving sector of the MSSM alone is sufficient to incorporate inflation. Since soft terms are not used in the construction, the scale of inflation can be made much higher, offering the benefits of a reduced fine tuning without losing the SUSY solution to the gauge hierarchy problem.

The construction begins with the superpotential for a fixed flat direction, Φ is

$$W = \frac{1}{2}M^2\Phi^2 + \sum_m \frac{\lambda_{3m}}{3m}\frac{\Phi^{3m}}{M^{2n-3}}.$$

Here we have explicitly included the cutoff scale M to highlight the dimensionless nature of the λ_i. M will typically be chosen to be at the Planck scale, M_P.

Let us first consider the case were W is entirely made of cubic terms, the first three of which are important. Let ϕ be the scalar part of Φ. The relevant $\mathcal{F}$-terms are,

$$\mathcal{F} = \lambda_1 \phi^2 + \lambda_2 \frac{\phi^5}{M^3} + \lambda_3 \frac{\phi^8}{M^6}.$$

Since $\mathcal{V}$ is just $|\mathcal{F}|^2$, critical points of $\mathcal{V}$ are also critical points of $\mathcal{F}$. Now the derivative of $\mathcal{F}$ with respect to ϕ is

$$\mathcal{F}_\phi = \phi \left(2\lambda_1 + 5\lambda_2 \frac{\phi^3}{M^3} + 8\lambda_3 \frac{\phi^6}{M^6} \right),$$

so critical points of $\mathcal{V}$ include $\phi = 0$ and,

$$\left(\frac{\phi_\pm}{M} \right)^3 = -\frac{5\lambda_2}{16\lambda_3} \pm \frac{1}{16\lambda_3} \left(25\lambda_2^2 - 64\lambda_1\lambda_3 \right)^{1/2}. \tag{V.2}$$

A degenerate critical point occurs when $\phi_+ = \phi_-$, which means that the discriminant of (V.2) vanishes,

$$25\lambda_2^2 - 64\lambda_1\lambda_3 = 0. \tag{V.3}$$

Without loss of generality, λ_1 can be made real by an appropriate rotation amongst the matter fields, and λ_2 can be absorbed into the definition of ϕ. This means

$$\lambda_3 = \frac{25\lambda_2^2}{64\lambda_1},$$

is always positive.

The scale of inflation impacts the observed spectrum of density perturbations. For definiteness, we take $M = M_P$. The degenerate critical points $\phi_\star$ of $\mathcal{V} = |\mathcal{F}|^2$ are

$$\phi_\star = \phi_0 e^{i\alpha}, \quad \alpha = \frac{\pi}{3}, \pi, \frac{5\pi}{3},$$

and

$$\phi_0 = \left(\frac{5}{16} \frac{\lambda_2}{\lambda_3} \right)^{1/3} M_P. \tag{V.4}$$

The Hubble parameter during inflation,

$$H_{inf} = \frac{9\lambda_1 \phi_0^2}{2\sqrt{30} M_P},$$

together with the cubic coupling at the inflection point,

$$\frac{1}{6} V_{\phi\phi\phi} = \frac{27\lambda_1^2 \phi_0}{5},$$

determine the normalization of the observed density perturbations,

$$\Delta_{\mathcal{R}} = \frac{V_{\phi\phi\phi} N_{\rm CMB}}{30\pi H_{\rm inf}} \approx 10^{-5}.$$

Here $N_{\rm CMB}$ is the number of e-foldings that took place between the modes which influenced CMB upon reentery and the end of inflation. Assuming a rapid transition from coherent oscillations to radiation domination — as one expects in MSSM inflation — one finds,

$$N_{\rm CMB} = 66.9 + \frac{1}{4}\log\left(V_0/M_P^4\right).$$

Putting all this together, agreement with observed normalization of the CMB power spectrum requires

$$\lambda_1 \left(\frac{16}{5}\frac{\lambda_3}{\lambda_2}\right)^{1/3} \sim \mathcal{O}(10^{-8}).$$

Since ϕ_0 must be less that M_P for the effective field theory to remain sensible, this and (V.4) lead to the upper bound

$$\lambda_1 \lesssim 10^{-8}.$$

This bound is saturated in the limit where ϕ_0 approaches M_P. Therefore, limit also corresponds to an upper bound on the scale of inflation,

$$H_{\rm inf} \lesssim 3 \times 10^9 \text{ GeV}.$$

At or just below this bound, contribution from TeV scale soft terms are clearly negligible. Indeed, any mass term less than 10^8 GeV or so will not affect the inflationary portion of $\mathcal{V}$. This is notable, as previous attempts to embed inflation in the MSSM used soft terms to tune the inflection point.

Let us make this concrete. For the specific choice of $\lambda_1 = 10^{-9}$ and $\lambda_2 = 10^{-6}$, we find $\lambda_3 \sim 10^{-3}$ and $\phi_0 \sim \frac{M_P}{10}$. This VEV is three orders of magnitude larger than previous MSSM-based scenarios, which helps to reduce the fine tuning in the inflection point. Let us compare more precisely with [92].

Parametrization the deformation away from a pure critical point by $\tilde{\alpha}$,

$$\tilde{\alpha} =_{\rm def} 1 - \frac{25\lambda_2^2}{128\lambda_1\lambda_3},$$

cf. the linear coupling in (II.17),

$$V_\phi = \frac{9}{5}\tilde{\alpha}\lambda_1^2\phi_0^3.$$

A slightly redshifted spectrum of density perturbations requires,

$$0 < \tilde{\alpha} \ll \frac{1}{N_{\rm CMB}^2}\left(\frac{\phi_0}{M_P}\right)^4. \tag{V.5}$$

In Ref. [92] ϕ_0 was three orders of magnitude smaller, meaning that the upper bound on $\tilde{\alpha}$ given in (V.5), was twelve orders of magnitude tighter! Therefore, our new prescription for SUSY-sector inflation offers an enormous improvement in the required fine tuning. The set of possible models is illustrated in Fig. V.1

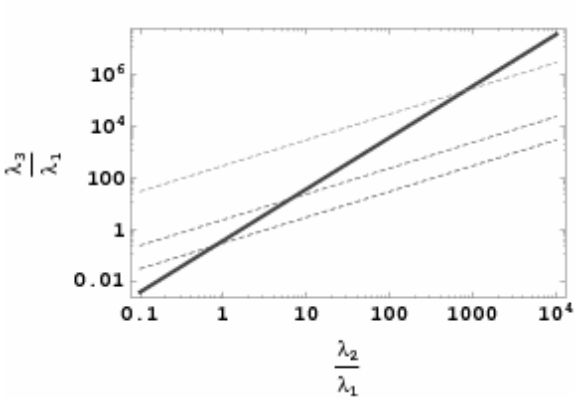

Figure V.1: The solid line represents the space of possible models, *i.e.* Eqn. (V.3). From bottom up, the dotted lines correspond to constant values of $\lambda_1 = 10^{-8}, 0.5 \times 10^{-9}, 10^{-9}$.

But this was just the minimal model. Inclusion of an additional higher order term, so that

$$\mathcal{F} = \lambda_1 \phi^2 + \lambda_2 \frac{\phi^5}{M^3} + \lambda_3 \frac{\phi^8}{M^6} + \lambda_4 \frac{\phi^{11}}{M^9},$$

leads to an upper bound [35] for $\tilde{\alpha}$,

$$0 < \tilde{\alpha} \ll \frac{1}{N_{\rm CMB}^{3/2}} \left(\frac{\phi_0}{M_P} \right)^3$$

Since the superpotential is fixed under renormalization group flow, the tuning between the couplings λ_i is protected. It is possible that the small number used to tune the inflection point could be related to other physical quantities, perhaps from the neutrino sector. In any case, the unnatural correlation between the SUSY preserving and SUSY breaking sector of the MSSM is no longer required. While many solutions to this problem have been proposed, this approach does not require any hidden sector dynamics, new symmetries or other as-yet any unknown physics. More importantly, this approach is completely generic within the realm of supersymmetric quantum field theories.

V.3 KKLT and the MSSM: Mirage Mediation

Models based on IIB flux compactifications have been studied extensively, particularly in KKLT class of models. Let us summarize the main ingredients. First, before stabilizing the moduli, the

compact space is assumed to be a compact Calabi-Yau, or an orientifold of the six-torus. There are technical differences between the two, which introduces extra complications and restrictions on the ingredients mentioned above. One such example is the one-cycle present in tori that does not survive when deformed to a proper Calabi-Yau (whose first cohomology group is trivial).

The internal space is assumed to be populated with D3-branes and D7-branes wrapping internal four-cycles. It is assumed that these branes fill the three spatial dimensions of our observed universe. The MSSM is comprised of fields restricted to these branes. Brane type will change the properties of the model.

The SUSY QFT model data for the four dimensional effective theory will be comprised of the Kähler potential, superpotential and the gauge kinetic function. Again we assume the presence of a single effective Kähler modulus, T. Respectively, these quantities are

$$\begin{aligned} K &= -3\log\left(-i(T-\bar{T})\right) + \sum_i Z_i(T,\bar{T})\overline{\Phi_i}\Phi_i, && \text{(V.6)} \\ W &= W_{\text{KKLT}} + \mathcal{Y}_{ijk}\Phi_i\Phi_j\Phi_k, && \text{(V.7)} \\ f_g &= T + f. && \text{(V.8)} \end{aligned}$$

Here a wavefunction renormalization factor $Z(T,\bar{T})$ connects the MSSM fields to the Kähler modulus T,

$$Z_i(T,\bar{T}) = \frac{1}{\left(-i(T-\bar{T})\right)^{n_i}}.$$

Here n_i is the modular weight of the chiral superfield Φ_i with respect to the $SL(2,\mathbb{Z})$ symmetry of the IIB theory. It is unity if Φ_i lives on a D3 brane; on a D7 it vanishes. The maganetic flux parameter f was found useful in [93] for finding low-scale models of inflation.

Recall that SUSY is broken by the contribution of the phenomenological, uplifting term $\mathcal{V}_{\text{pheno}}$. This generates an $\mathcal{F}$-term for the scalar field T,

$$F_T = e^{K/2}D_T W. \qquad \text{(V.9)}$$

With out the uplift, this is a supersymmetric local minimum of the theory with an negative vacuum energy — SUSY AdS space. After the uplift, there is a very small, positive amount of vacuum energy. Therefore, there are two schemes by which SUSY breaking is communicated to the fields Φ_i: **anomaly mediation** and moduli mediation. The former is generically present when lifting AdS vacua, and the latter derives from the non-vanishing F_T in (V.9).

Anomaly mediation gives a soft mass to the gauginos at the EFT cutoff, presumably the GUT scale, of the form,

$$M_{\text{anomaly}} = \frac{m_{3/2}}{16\pi^2} b g^2. \qquad \text{(V.10)}$$

Here g is the Yang-Mills coupling under which the gaugino is charged. b is the beta function for that particular coupling and $m_{3/2}$ is the gravitino mass — the standard proxy for the scale of

SUSY breaking.

The **moduli mediation** contribution to SUSY breaking is parametrized by F_T. Here the contribution to the gaugino soft mass is,

$$M_T = F_T \partial_T \log \mathrm{Re}(f_g). \tag{V.11}$$

There are also soft masses for the scalars and trilinear couplings, which are parametrized in terms of Z_i,

$$m_i^2 = -F^T F^{\bar{T}} \partial_T \partial_{\bar{T}} \log\left(Z_i e^{-K/3}\right), \tag{V.12}$$

$$A_{ijk} = F^T \partial_T \log\left(e^{-K} Z_i Z_j Z_k\right). \tag{V.13}$$

Note that we evaluate K without the contributions of Φ in computing the above quantities — at least to first order.

Having multiple sectors of SUSY breaking can lead to phenomenologically interesting consequences. In particular, the ratio of anomaly to moduli mediated SUSY breaking parametrizes can cause the gaugino masses to unify at much lower energies than the GUT scale. Precision electroweak experiments at the LHC, if gauginos are observed, may serve as boundary conditions for a renormalization group analysis that can observe such effects. Collectively, these effects are referred to as **mirage mediation**.

The ratio of these effects is typically parametrized by the ratio of gaugino soft mass contributions,

$$\alpha_{\mathrm{mirage}} = \frac{M_{\mathrm{anomaly}}}{M_T}. \tag{V.14}$$

V.4 A_4 Parameters and Mirage Mediation

As discussed in Section III.3.2, single field racetrack inflation belongs to the A_4 class of models. The potentials have three independent couplings, and therefore the inflationary models are two-parameter families governed by the moduli space $\mathcal{M}_{A_4}$. A cross-section of $\mathcal{M}_{A_4}$ is depicted in Fig. IV.5. It is convenient to parametrize this model by its three critical points: the inflection point α, the meta-stable vacuum at β and the barrier to decompactification at γ. Note that in our parametrization,

$$2\alpha + \beta + \gamma = 0.$$

Now, the height of the potential during inflation scales as

$$\mathcal{V}(\alpha) \propto (\beta - \alpha)^4 (\gamma - \alpha),$$

and the height of the barrier,

$$\mathcal{V}(\gamma) \propto \alpha \left[(\beta - \alpha)^3 - (\gamma - \alpha)^3 \right]. \tag{V.15}$$

$\mathcal{V}(\alpha)$ serves as a proxy for the scale of inflation and $\mathcal{V}(\gamma)$ serves as a proxy for the scale of SUSY breaking. Note also that $\mathcal{V}(\alpha)$ enters into the normalization of the power spectrum of density perturbations (II.35),

$$\Delta^2_{\mathcal{R}} = \frac{\mathcal{V}(\alpha)}{12\pi^2} N_e^4 Z^2 (\beta - \alpha)^2 (\gamma - \alpha)^2, \tag{V.16}$$

where $H^2 \approx \mathcal{V}(\alpha)/3$.

While such scaling is only exact when these three critical points nearly degenerate — *i.e.* at extremely low scales — it will hold approximately when any of the critical points is too small (*i.e.* the VEV σ) is much larger than one, which coincides with the supergravity approximation. This can be guaranteed, for instance, when f is large.

Assuming the generic case where the critical point VEVs α, β, γ approximately equivalent in magnitude, one finds that the SUSY breaking order parameter (V.9) is

$$F_T = \frac{16\pi\alpha^3 |\Delta_{\mathcal{R}}|^2}{3N_e^2 |(\beta - \alpha)(\gamma - \alpha)|},$$

where (V.16) was employed.

Weak scale SUSY occurs when σ has come to rest in the vacuum at β. The gaugino mass then picks up a moduli mediation contribution from (V.11),

$$M_T = \frac{8\pi |\Delta_{\mathcal{R}}|^2 \alpha^3}{3N_e^2 |(\beta - \alpha)(\gamma - \alpha)|(\beta - f)}. \tag{V.17}$$

The anomaly contribution (V.10) is

$$M_{\text{anomaly}} \propto \frac{\sqrt{\mathcal{V}(\gamma)}}{M_P}, \tag{V.18}$$

so using (V.17) and (V.15) the mirage mediation parameter (V.14) is

$$\alpha_{\text{mirage}} = \frac{\beta - f}{32}.$$

All together, the gaugino mass should read,

$$M = \frac{8\pi |\Delta_{\mathcal{R}}|^2 \alpha^3}{3N_e^2 |(\beta - \alpha)(\gamma - \alpha)|(\beta - f)} (1 - \frac{b g^2}{16\pi^2} \alpha_{\text{mirage}} \log \left[\sqrt{\mathcal{V}(\gamma)} \right]) \tag{V.19}$$

A few comments are in order. First, observations place $|\Delta^2_{\mathcal{R}}| \sim 10^{-5}$, M_0 is around $(10^{-4} -$

$10^{-2})M_P$. This range runs down to 100-1000 GeV. These values can of course be raised by increasing the separation $\beta - \gamma = 2(\alpha + \beta)$. Second, α_{mirage} — a potential precision electroweak observable at the LHC — is set by the value of β. Therefore, if α can be determined, perhaps by measuring the scale of inflation in some way, the details of the A_4 potential can be observationally determined. So concludes our example of how to the considerations of Chapter IV can be used to study, observe and constrain the embeddings of inflation into particle physics.

CHAPTER VI

FIXED POINTS IN PHASE SPACE

VI.1 The Likelihood of Inflation

VI.1.1 The Trouble with Attractors

The attractor dynamics which drives the gravity-scalar system towards inflationary trajectories is sometimes credited with helping inflation become a predictive theory [94]. For a given potential, the fact that a large portion of parameter space can be drawn to the slow-roll trajectory, as detailed in Chapter II.1.3, lends support to the generic universe paradigm. Recent Planck results [9] are consistent with the "vanilla" model of single field, slow-roll inflation. Such observations can rightly be used to bolster inflation as a predictive theory which explains the origin of our universe.

Despite these successes, the subject of inflation resists closure. Without meaningful correlation between inflationary dynamics and particle physics the picture is incomplete; the inflaton is a hanging gauge singlet. The mystery of how inflation embeds into larger theory of particle physics — or even string theory — is in itself an interesting open question. But such concerns only hint at larger questions. Further investigation reveals consistency problems with the attractor-as-predictor philosophy.

The problem is that successful inflation requires fifty or so e-foldings of inflation; the universe must have been on the slow-roll trajectory for a sufficient duration. Because we know nothing about the conditions which generated inflation, it is this large number which unravels the effectiveness of the attractor argument.

Attempts to rigorously determine of the likelihood of successful inflation typically require investigating entire trajectories. In attractor dynamics, the density of states decreases with proper time. Therefore any attempt to assign a statistical weight to a collection of trajectories is necessarily time dependent. For macroscopic, open systems, the attractor dynamics can be tied to energy loss. Therefore it is subject to the laws of thermodynamics, and this phenomena causes no conceptual problems. Kofman, *et. al.* argue that inflation is inevitable by draw parallels with the second law of thermodynamics [49]. Just as the shards of glass below the dining table can be taken as evidence of a highly entropy generating event, so too is the size of our universe, replete with its observed perturbations, indicative of a period of inflation.

One could rightly argue that the universe is a closed system, and since its is based on fundamental, quantum fields, CPT should be respected. Of course, the rolling scalar field spontaneously breaks time-translation invariance, and the cosmic fluctuations are just those associated to the Nambu-Goldstone mode associated to this symmetry breaking [29]. Because time translation

invariance is restored microscopically, a number of authors [95, 96, 97, 50, 98] have studied the Liouville measure. One is then tasked with picking the appropriate time to evaluate the density of states and ask statistical questions.

These conflicting perspectives lead to mutually antithetical conclusions, and neither is above reproach. In the first case, the all important initial conditions must be accounted for — not unlike the extremely low energy state of a wine glass perched on a table. In the second case, running the density of states backwards without somehow accounting for the Nambu-Goldstone phenomena remains to be rigorously justified. Worse, one is left to explain why the likelihood of our own universe is suppressed by a factor of e^{-150} [50].

Our discussion will not solve this conceptual problem, but offer instead a third way. The attractor dynamics special to inflection point inflation reduce the exponential time-dependence of the density of states to something exponentially close to a Heavyside Θ-function.

VI.1.2 Likelihoods, Probabilities and All That

To facilitate our discussion of genericity in the multiverse ensemble, we briefly discuss the basic ideas of Bayesian statistics in the context of inflationary cosmology.

The we employ notion of a multiverse from [50]. Denoted by $\mathbb{M}$, the **multiverse** is defined to be the set of individual trajectories in the gravity-scalar phase space. To specify $\mathbb{M}$ one must also specify a theory to work in, typically represented by a Lagrangian $\mathcal{L}$. When precision is needed, we specify this particular multiverse by $\mathbb{M}(\mathcal{L})$. To promote $\mathbb{M}$ a statistical ensemble, a probability measure is required. The ambiguity in choosing such a measure is the subject of this chapter, and we will define and apply different measures in the following sections. For the moment, let us simply assume that one such measure exists, is well-defined and applied.

Let $\mathcal{P}(\mathcal{A})$ denote the probability of a given event $\mathcal{A}$. Often conditional probabilities are of interest. The conditional probability that an event $\mathcal{A}$ occurs given that event $\mathcal{B}$ is $\mathcal{P}(\mathcal{A}|\mathcal{B})$.

$\mathcal{P}(\mathcal{A}|\mathcal{B})$ and $\mathcal{P}(\mathcal{B}|\mathcal{A})$ are generally different, and related by Bayes' equation,

$$\mathcal{P}(\mathcal{A}|\mathcal{B}) = \frac{\mathcal{P}(\mathcal{A})\mathcal{P}(\mathcal{B}|\mathcal{A})}{\mathcal{P}(\mathcal{B})}.$$

In the context of inflation, the probability of successful inflation is a precise quantity, $\mathcal{P}(\mathcal{U}|50)$. Namely, what is the conditional probability of finding a universe $\mathcal{U} \in \mathbb{M}$ in which fifty e-foldings have occurred. To define this quantity, we must first define $\mathcal{P}(50)$, $\mathcal{P}(\mathcal{U})$ and $\mathcal{P}(50|\mathcal{U})$.

The probability of living within a specific universe $\mathcal{U}$ is $\mathcal{P}(\mathcal{U})$. This amounts to specifying the Cauchy data for the field equations, *i.e.* the boundary conditions. Without knowledge of the ultraviolet physics which give rise to inflation, $\mathcal{P}(\mathcal{U})$ is unknown. We must put it in by hand. This is a common feature of Bayesian analysis, and such subjective inputs are called priors. Without

a large number of universes to empirically study $\mathcal{P}(\mathcal{U})$, our only recourse is the democratic one: all boundary conditions are equally possible. $\mathcal{P}(\mathcal{U})$ is constant.

$\mathcal{P}(50)$, which can be tautologically expanded as,

$$\mathcal{P}(50) = \sum_{u \in \mathbb{M}} \mathcal{P}(u)\mathcal{P}(u|60),$$

amounts to a normalization of the overall conditional probability $\mathcal{P}(\mathcal{U}|50)$, as we shall demonstrate explicitly later in this chapter.

The quantity $\mathcal{P}(50|\mathcal{U})$ is a posterior probability; we compute it from the details of the physical model. It is often called a likelihood function. Therefore, when one asks to compute the likelihood of fifty e-foldings of inflation, this is the quantity of interest.

VI.1.3 An Escape through the Landscape

So far we have considered $\mathcal{U}$ as a distinct trajectory in phase space, with a fixed Lagrangian. Allowing $\mathcal{L}$ to vary represents a significant extension of the ensemble of possible universes. Were a class of inflationary models with sufficient inflation and without a fine tuning of the initial conditions to exist, a modification of the conclusions of [50] would be in order. As we shall demonstrate in this chapter, inflection point inflation is such a class.

Whether or not the landscape exists, it may be very possible that string theory offers a large number of de Sitter solutions in which inflation could have occurred. At the very least, there is a plethora of field theory models in which inflation is embedded into particle particle physics like the MSSM. Coarse-grainning over either of these solution sets is always possible provided inflation can be explained as an effective field theory, which is certainly a conservative assumption.

Because we have limited ourselves to canonical scalar fields, the set of possible Lagrangians can be reduced to the set of possible scalar potentials. This restriction is well motivated by the recent results from the Planck Collaboration [9], which suggested that inflation is in good agreement with single field, slow roll inflation in a shallow potential. Indeed, the non-observation of significant nongaussanity has ruled out many of the exotic opportunities for new physics.

In what follows we will compute the likelihood of inflation for the various ADE models of inflection point inflation, and find that the likelihood obeys a power law

$$\mathcal{P} \propto \frac{1}{N_e^3}.$$

In particular, we derive this scaling behavior as a property as coming from a single field limit of an inflection point model.

VI.2 Phase Space of the Gravity-Scalar System

The action for the gravity-scalar system is

$$S = \int d^4x\, \mathcal{L} = \int d^4x\, \sqrt{-g} \left(\frac{R}{2} + \frac{1}{2} g^{\mu\nu} \partial_\mu \phi \partial_\mu \phi - \mathcal{V} \right).$$

which can be put into ADM form,

$$S = S_{\text{ADM}} + S_{\text{scalars}}.$$

Here S_{ADM} is the Einstein-Hilbert action in ADM form (II.21), and

$$S_{\text{scalar}} = \frac{1}{2} \int d^4x \frac{\sqrt{\gamma}}{\mathfrak{N}} \left[(\frac{d\phi}{dt} - \mathfrak{N}^i \partial_i \phi)^2 - \mathfrak{N}^2 \gamma^{ij} \partial_i \phi \partial_j \phi - 2\mathfrak{N}^2 V \right].$$

The generalization to multiple scalar fields is straight forward. The background dynamics are subject to the usual condition of spatial uniformity, which simplifies this to

$$S_{\text{scalars}} = \frac{1}{2} \int d^4x \frac{\sqrt{\gamma}}{\mathfrak{N}} \left[\left(\frac{d\phi}{dt} \right)^2 - 2\mathfrak{N}^2 V \right]. \tag{VI.1}$$

For a single, canonical scalar field, phase space is spanned by the coordinates $\mathfrak{N}$, a and ϕ and the associated canonical momenta, p_N, p_a and p_ϕ, respectively. For a coordinate q^Σ, the canonical momentum p_Σ is defined by

$$p_\Sigma = \frac{\delta \mathcal{L}}{\delta \dot{q}^\Sigma}.$$

The Ricci scalar associated to the FLRW metric is,

$$R = 6 \left[\frac{\ddot{a}}{a} + \left(\frac{\dot{a}}{a} \right)^2 + \frac{k}{a^2} \right],$$

and $\det g = a^3$. Integrating the Einstein-Hilbert term by parts,

$$\frac{1}{2} \int d^4\ R = 3 \int d^4x\, a^3 \left(-H^2 + \frac{k}{a^2} \right).$$

Curiously, the action in terms of the scale factor looks like the kinetic term for a moduli field — as it should, since it is a geometric modulus — only with the wrong sign. This will play an important role in what follows.

We are now in a position to compute the various p_Σ,

$$p_{\mathfrak{N}} = 0, \tag{VI.2}$$
$$p_a = -6a^2H, \tag{VI.3}$$
$$p_\phi = a^3\dot{\phi}. \tag{VI.4}$$

The Hamiltonian of this system is,

$$\mathcal{H} = \mathfrak{N}\left(-\frac{p_a^2}{12a} + \frac{p_\phi^2}{2a^3} + a^3\mathcal{V} - 3ak\right).$$

The equation of motion for $\mathfrak{N}$ is then,

$$p_a^2 = \frac{6p_\phi^2}{a^2} + 12a^4\mathcal{V} - 36a^2k \tag{VI.5}$$

So $\mathcal{H}$ vanishes, as is often the case for systems with an unfixed gauge symmetry. The resulting constraint equation is simply the Friedmann equation, (II.2). As above, we set k to zero for simplicity unless otherwise specified.

VI.3 The Liouville Measure and the Ensemble Multiverse

Knowing that the lapse function $\mathfrak{N}$ is an auxiliary field, our configuration space for the gravity-scalar system is the space of all pairings (ϕ, a). We can model this as the upper half plane of $\mathbb{R}^2$, since we typically consider only positive a.

The canonical one-form on $T^\star Q$ is

$$\theta = p_a\,da + p_\phi\,d\phi,$$

which defines the symplectic form

$$\omega = d\theta.$$

The Friedmann constraint means that one of these coordinates in determined in terms of the other three. This selects a subvariety $\mathcal{P}_Q \subset T^\star Q$ as the constraint hypersurface or physical phase space. There is some freedom in choosing where to apply this constraint. When the system is fast-rolling, it is helpful to fix p_ϕ. For slow-roll inflation, it is more practical to fix p_a by explicitly plugging in (VI.3) and evaluating. This, or alternatively by solving (VI.5).

In this case

$$\theta = -6Ha^2\,da + p_\phi\,d\phi,$$

so that

$$d\theta = \frac{\partial p_a}{\partial \phi}\,d\phi \wedge da + \frac{\partial p_a}{\partial p_\phi}\,dp_\phi \wedge da + dp_\phi \wedge d\phi,$$

or

$$d\theta = -6a^2 \frac{\partial H}{\partial \phi} d\phi \wedge da - 6a^2 \frac{\partial H}{\partial p_\phi} dp_\phi \wedge da + dp_\phi \wedge d\phi.$$

The density of states is often given by the Liouville measure on phase space, which for a $2n$ dimensional phase space is just n wedge products of the symplectic form. In three dimensions on can integrate by parts to find the volume form on $\mathcal{P}_Q$ to be

$$\mathbb{V}_3 = \theta \wedge d\theta = \left(p_a - \frac{\partial p_a}{\partial p_\phi} p_\phi \right) dp_\phi \wedge d\phi \wedge da,$$

or

$$\mathbb{V}_3 = \frac{2a^2 \mathcal{V}}{H} dp_\phi \wedge d\phi \wedge da.$$

In terms of the flow coordinate N, we find

$$\mathbb{V}_3 = e^{3N} \frac{2\mathcal{V}}{H} dp_\phi \wedge d\phi \wedge dN, \tag{VI.6}$$

which gives the characteristic dependence of this volume on the number of e-foldings of expansion, N.

When viewed from this perspective, $\mathcal{P}_Q$ is a contact manifold, with θ being the contact 1-form. This observation has far-ranging consequences for the ensemble of inflationary universes.

For symplectic manifolds, Liouville's theorem says that any volume form is invariant under Hamiltonian flow. The Liouville measure or volume form for a symplectic manifold of dimension $2n$ is the n-fold wedge product of the symplectic form ω. An analog of Liouville's theorem exists for contact manifolds, with one important caveat. Here, the volume form is as in (VI.6). For higher dimensional contact manifolds, more wedge products of $d\theta$ are required. The crucial caveat in Liouville's theorem for contact manfolds is that the volume form of a contact manifold is preserved under Reeb (Hamiltonian) flow *up to a conformal factor.* This explains the peculiar feature of (VI.6).

For us, this means that the volume of phase space grows as the universe evolves. This simple fact helps to explain the observations in [96], where the likelihood of successful inflation was strongly dependent on when the measure was applied. Indeed, the interpretation of $\mathcal{P}_Q$ as a contact manifold immediately gives results which were painstaking derived by analogy with three dimensional electromagnetism in [50].

In later sections we shall discuss the application of this measure by Gibbons and Turok which resulted in an exponentially suppressed likelihood of inflation,

$$\mathcal{P} \propto e^{-3N_e}, \tag{VI.7}$$

although the ambiguity already appears with the N dependence in (VI.6). With this ambiguity explained in terms of the natural contact structure on phase space, there is a need to replace it

with something which admits a reasonable physical interpretation.

VI.4 Dynamical Fixed Points

VI.4.1 Effective Dissipation of Scalar Field Energy

In what follows it is helpful to be slight more general. For N canonical scalar fields, defined the quantity

$$\Upsilon = \sum_{A=1}^{N} \phi_A'^2,$$

which is essentially the fraction of the Hubble scale comprised of kinetic energy. The total energy density of the scalar fields is

$$\rho = \frac{V}{1 - \frac{1}{6}\Upsilon}. \tag{VI.8}$$

To see how it evolves with metric expansion we compute

$$\rho' = \sum_{A=1}^{N} \frac{V_{\phi_A}\phi_A'}{\left(1 - \frac{1}{6}\Upsilon\right)} + \frac{V\phi_A'\phi_A''}{3\left(1 - \frac{1}{6}\Upsilon\right)^2},$$

Making use of (II.3), (II.6) and (VI.8) one finds,

$$\rho' = \sum_{a=1}^{N} \frac{\rho\phi_A'}{1 - \frac{1}{6}\Upsilon}\left[\left(1 - \frac{1}{6}\Upsilon\right)\frac{\partial \log \mathcal{V}}{\partial \phi_A} - \left(1 - \frac{1}{6}\Upsilon\right)(\phi_A' + \frac{\partial \log \mathcal{V}}{\partial \phi_A})\right],$$

which simplifies to

$$\rho' = -\Upsilon\rho. \tag{VI.9}$$

While the total energy is not lost, the expansion of spacetime redshifts the kinetic energy of the scalar fields. It is possible that the kinetic energy of the fields may be completely redshifted away before the fields find the global minimum of the potential. In particular, they may come to rest at an inflection point. As we review below, this is in fact realized in inflection point models, and lends new physical perspective to the work of Itzhaki and Kovetz.

VI.4.2 The Itzhaki-Kovetz Model

In [36], Itzhaki and Kovetz investigated a curious property of the gravity-scalar system subject to the inflection point potential,

$$\mathcal{V}_{IK} = \beta\phi^3 + 1.$$

Starting from rest above the degenerate critical point, they let the scalar field roll down the potential and found that the behavior of the trajectories depended strongly on value of the coupling

β. Specifically, if β is below a certain critical value,

$$\beta_C \approx 0.774,$$

the scalar field asymptotically approaches the critical point in the limit $N \to \infty$. This is an inflationary solution, for which H asymptotically approaches a constant — *i.e.* de Sitter space. For β greater than β_C, ϕ overshoots the inflection point in a finite time and only a small amount of inflation occurs.

They framed this observation as a phase transition between chaotic and inflection point inflation, and demonstrated that with $1/N_e$ e-foldings of inflation being the order parameter, it replicates the physics of a second order phase transition. In this context, this can be viewed as manifestation of "critical slowing down" in the gravity-scalar system near an inflection point. What is perhaps most important is their study deformations to $\mathcal{V}_{IK}$

Irrelevant and marginal operators, like ϕ^4, did not effect the qualitative behavior seen here. Relevant operators like ϕ and ϕ^2, did. The former case is just an example of finding an A_2 model nested within some larger construction. Indeed, we shall consider the A_3 case — and find similar behavior — shortly. The latter case is important. While any deformation ruins the fixed point behavior, for sufficiently small relevant couplings, $1/N_e$ varies parametrically with them. In other words, the existence of the fixed point has a residual effect in the deformed theory.

This is precisely what you would expect from (II.19), where N_e depend on the linear coupling λ as

$$N_e \propto \frac{1}{\sqrt{\lambda}}.$$

The point is that inflection points are extremely efficient attractors. So long as couplings like β are in the appropriate regime, inflation is virtually guaranteed. The number of e-foldings of inflation varies with couplings such as λ. Note that N_e may be much larger, perhaps if a period of chaotic inflation occurred before ϕ approached the inflection point.

Finally we lend a different physical perspective on the existence of these the fixed point. Recall from (**??**) that $\mathcal{V}_{IK}$ enters the field equations as logarithmic derivative. This means its overall scaling of is irrelevant for dynamics. Let us then write

$$\mathcal{V}_{IK} = \beta \left(\phi^3 + \frac{1}{\beta} \right).$$

Up to an overall scaling, the energy density of ϕ is proportional to $1/\beta$. Appealing to (VI.9), we see that the dissipation of ρ is proportional to ρ itself. Therefore, for sufficiently large $1/\beta$, all the kinetic energy redshifts from ϕ as it approaches the inflection point. Sufficiently large here is then $1/\beta_C$. If β is too large, its reciprocal is too small and the kinetic energy does not redshift enough to avoid overshooting the inflection point.

VI.4.3 The Basin of Attraction for the A_3 Model

The Itzhaki-Kovetz model demonstrated that inflection point inflation is viable for virtually all initial field configurations. In Ref. [37] we extended this analysis to all of phase space, proving that under certain assumptions, the likelihood of inflection point inflation occurring is exponentially close to a yes-no question.

We demonstrate these ideas with an A_3 class of inflection point model. Repeating the analysis of Itzhaki and Kovetz with the potential,

$$\mathcal{V} = \frac{1}{4}\phi^4 + \alpha\phi^3 + \frac{27}{4}\alpha^4, \tag{VI.10}$$

one finds a critical value of the cubic coupling

$$\alpha_C \approx 0.661.$$

Above α_C, the ϕ attracts to the inflection point. Below α_C is overshoots.

Despite this apparent reversal, it is the same physics as in the Itzhaki-Kovetz model. The constant term in (VI.10) is chosen so that the vacuum energy vanishes at the global minimum of $\mathcal{V}$, located at $\phi = -3\alpha$. It is also the energy density during inflection point inflation.

Better still, α_C is just the tip of the proverbial iceberg. While arbitrary initial position above the inflection point attracts for all $\alpha \geq \alpha_C$, the same is not true for arbitrary initial velocity. For a given value of α, there is a basin of attraction in phase space to the inflection point; sufficiently large initial ϕ' will cause an overshoot. At α_C, the basin starts from a line in $\mathcal{P}$ along the initial ϕ direction. α increases, the basin opens into the initial ϕ' direction exponentially.

Owning to the universality associated to the breaking of an A, D or E-type potential down to a single field, A_2 limit, the qualitative features discussed here hold true for all models of inflection point inflation.

VI.4.4 Multifield Fixed Points

Inflection points can still be fixed points in models were multiple fields are important. While the phase space enlarges to $(2N+1)$-dimensions for N scalars, the details are only slightly modified. One interesting feature of multifield fixed points is the existence of a new parameter: the mixing angle between initial configurations of the two fields.

To see this, let us consider the D_5 model with the A_3 limit discussed above.

$$\mathcal{V} = \frac{1}{4}\phi^4 + \alpha\phi^3 + \frac{1}{2}\chi^2\phi + \alpha\chi^2 + \frac{27}{4}\alpha^4.$$

To make this potential somewhat more physical, we append two deformations. First, a small tadpole at the inflection point to ensure finite e-foldings, an in (II.19). Next, we increase the mass

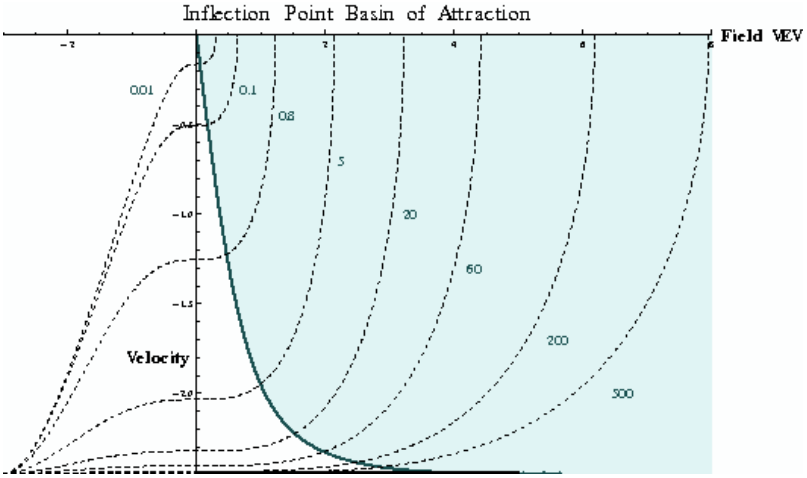

Figure VI.1: The basin of attraction in a projection of phase space to the (ϕ, ϕ')-plane for the inflection point of the A_3 potential is shown for $\alpha = 1$ and $\lambda = 0$. The horizontal axis shows VEVs above the point of inflection, which itself is located at the origin. Note that in this parametrization, $\phi' = -\sqrt{6}$ corresponds to complete kinetic energy domination. Field velocities away from the inflection point, thought not explicitly shown, are within the basin of attraction.

of the spectator field χ to allow for a stable local minimum.

$$\frac{1}{4}\phi^4 + \alpha\phi^3 + \frac{1}{2}\chi^2\phi + \lambda\phi + \frac{1}{2}(6\alpha + m_\chi^2)\chi^2 + \left(\frac{27}{4}\alpha^4 - 3\lambda\alpha\right). \tag{VI.11}$$

The form of the term $\frac{1}{2}(6\alpha + m_\chi^2)\chi^2$ is a convention, chosen so that vanishing m_χ corresponds to a flat direction for χ at the critical point $(\phi, \chi) = (-3\alpha, 0)$. Note that this is an example of an exceptional degenerate critical point which would be lifted in general by higher order terms. In any case, with χ starting from rest at zero VEV, this model exactly replicates the single-field A_3 model, at least in term sof the background FLRW and VEV dynamics.

Now let us consider the effect of mixing the initial conditions.

$$\mathcal{V} = \frac{1}{4}\phi^4 + \alpha\phi^3 + \frac{1}{2}\chi^2\phi + \alpha\chi^2 + \beta\chi + \lambda\phi + \frac{27}{4}\alpha^4.$$

Let us parametrize the Cauchy data for the two scalar fields x and y as follows. The initial position of the fields shall be parametrized by a distance in field space r_0 and a mixing angle θ.

$$x_0 = r_0 \cos\theta_r, \quad y_0 = r_0 \sin\theta_r. \tag{VI.12}$$

The initial velocities can be similar parametrized,

$$x_0' = v_0 \cos\theta_v, \quad y_0' = v_0 \sin\theta_v, \tag{VI.13}$$

where,

$$x_0' = \frac{dx}{dN}\Big|_{x=x_0}, \quad y_0' = \frac{dy}{dN}\Big|_{y=y_0}.$$

Some example trajectories are shown in Fig. VI.2. Here, different angles $\theta_r = -0.2\pi, 0.1\pi, 0.3\pi$ are shown all to attract towards the approximate inflection point. Upon reaching the inflection point, all three trajectories merge to to approach the metastable vacuum along the same, slow-roll trajectory.

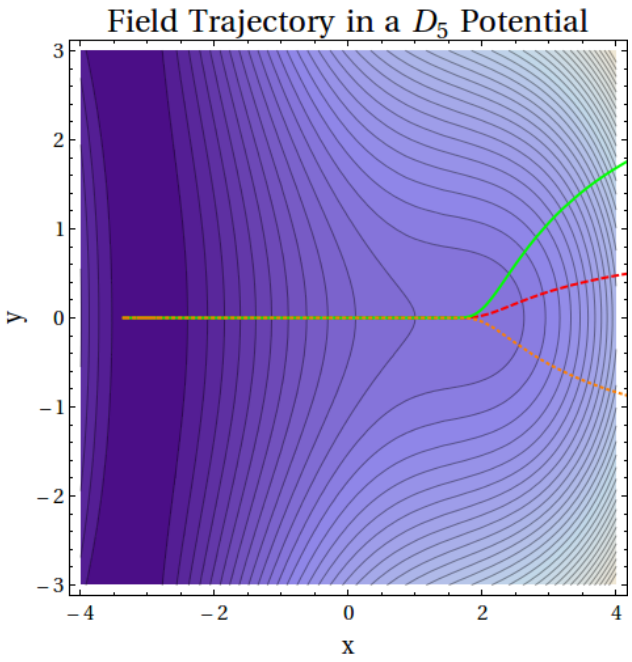

Figure VI.2: The D_5 model potential is shown with three separate trajectories being attracted towards the nearly degenerate critical point. There is not mixing, but non vanishing λ from (VI.11) causes inflation to end by falling in a local minimum.

These effects can also be observed for $\beta \sim \mathcal{O}(1)$. Allowing for a linear term in χ essentially rotates the eigenvectors of the Hessian, meaning that the inflaton is a nontrivial mixture of ϕ and χ. This can be interpreted as a torsional distortion of the potential in field space, and the basin of attraction of the inflection point is similarly rotated. This effect is seen in Fig. VI.3, where various initial angle are employed, and the trajectories are not symmetric under $\theta_r \to -\theta_r$. Note, however, that those trajectories which are attracted to the inflection point again follow the same slow-roll trajectory towards a local minimum (or a runaway, depending on the potential). Whereas those that overshoot necessarily run off in the other direction.

Some previous work on fixed point in cosmological scalars was given in Ref. [99], although it focused on late-time, runaway scenarios. Unifying the inflection point analysis with these techniques may be interesting in understanding general features of gravity-scalar dynamics.

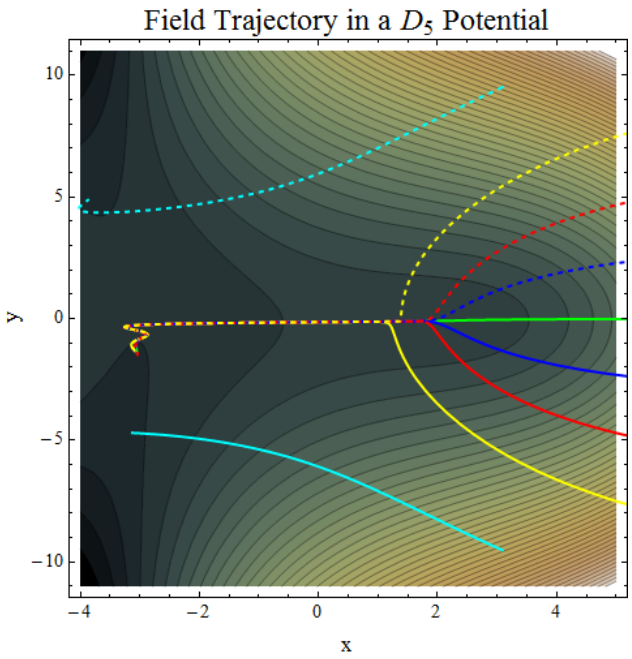

Figure VI.3: Trajectories in the D_5 potential starting at rest ($v_0 = 0$) with initial position parametrized by Eqn. (VI.12) with $\theta_r = 0, \pm 0.1\pi, \pm 0.2\pi, \pm 0.3\pi, \pm 0.4\pi$. With nonzero mixing parameter c, the basin of attraction has shifted slightly clockwise. Notice the asymmetry present between $\pm\theta$. Note that all trajectories within the basin of attraction fall to the lower valley of the potential.

VI.4.5 Fixed Points Violate Slow-Roll

We close this section with a final observation about the fixed point behavior. In the vicinity of an inflection point, the slow-roll trajectory

$$\phi' = -\frac{\partial \log V}{\partial \phi},$$

brakes abruptly before asymptotically towards the de-Sitter solution. This braking is to sharp to be physical; the inflaton momentarily hopes out of slow-roll before it begins the asymptotic approach to the inflection point. Even if said inflection point is slightly deformed by relevant operators, this breaking is too strong to be physical.

As one might expect, near the boundary of the basin of attraction the disparity between the slow-roll solution and the physical one grows sharply. Eventually the braking required by slow-roll becomes too strong, and the system overshoots.

The precise behavior is even more subtle. To visualize this, we define the parameter Ξ as

$$\Xi =_{\text{def}} \frac{\phi''}{\phi'}.$$

Near the boundary of the basin of attraction, the spike in Ξ can be $\mathcal{O}(1)$. Curiously, it saturates at three (precisely the same three in Eqn. (II.10)). Moreover, the duration of the spike can easily be $N \sim \mathcal{O}(1)$. As such, one must take care as these effects can manifest in the study of the cosmological perturbations. Indeed, in Chapter VII we shall use this fact to our advantage to explain an anomaly in the CMB data.

VI.5 The Cosmological Measure Revisited

VI.5.1 Exponential Suppression from the Liouville Measure

In [50] Gibbons and Turok sought to retrofit the Liouville measure first studied in [96, 97]. Aside from the apparent time dependence of the measure (VI.6), it was also badly divergent. They employed a natural cutoff on this measure by coarse grainning over observably indistinguishable spacetimes. More precisely, all universes whose spatial curvature Ω_k was too small to be observed were identified with $k = 0$. This suppresses many of solutions which were inflated to large size, and one might naïvely worry that this is the cause of the exponential suppression (VI.7) of the likelihood. Closer inspection reveals this is not the case. Indeed, the ensemble of late-time trajectories is dominated by those that were fast-rolling in the recent past. This is just attractor dynamics in reverse. In their terms, the divergence represented the invariance of the FLRW metric to a rescaling of a. In this sense their cutoff was a projectiviation of the naïve $\mathbb{M}$.

VI.5.2 Enlarging the Ensemble

The analysis Gibbons and Turok was done for a quadratic potential, although their results hold most of the time for chaotic inflation on a smooth, monotonic potential. In the same way a wine glass focuses light, degenerate critical points of the potential can create caustics in phase space which focus trajectories towards inflection point inflation. These surprising effects were not considered in [50].

Incorporating these details into the computation of $\mathcal{P}(N_e|\mathcal{U})$ extends $\mathbb{M}$ to include an ensemble of possible couplings from a specific class of potentials $\mathcal{M}_\mathcal{V}$ as studied in Chapter IV. Since each model has a single parameter which controls the number of e-foldings of inflation (*cf.* λ_1 of (II.19)), we shall see that the power law likelihood $1/N_e^3$ is universal to all ADE model classes, at least for sufficiently large N_e (*i.e* fifty).

To make this analysis concrete, we choose $\mathcal{V}$ to be of A_3 type. Recall that such a potential is given by

$$\mathcal{V} = \frac{1}{4}x^4 + \frac{a}{2}x^2 + bx + \text{constant}.$$

Recall that for the A_3 model, a critical point exists when

$$\left(\frac{a}{3}\right)^3 + \left(\frac{b}{2}\right)^2 = 0. \tag{IV.12}$$

A slight deformation away from this condition gives,

$$\left(\frac{a}{3}\right)^3 + \left(\frac{b+\lambda}{2}\right)^2 = 0. \tag{VI.14}$$

About the inflection point α, the potential is

$$\mathcal{V} = \frac{1}{4}(x-\alpha)^4 + \alpha(x-\alpha)^3 + \lambda(x-\alpha) + \frac{27}{4}\alpha^4 + \mathcal{O}(\lambda).$$

From (II.19), we can write λ in terms of the number of e-foldings of inflection point inflation, N_e,

$$\lambda = \frac{\pi^2}{8N_e^2\sqrt{3a}}.$$

Therefore, we can define a curve of constant N_e in $\mathcal{M}_{A_3}$ as

$$b(a) = -2\left(\frac{a}{3}\right)^{3/2} + \frac{\pi^2}{8N_e^2\sqrt{3a}}. \tag{VI.15}$$

Let γ_{N_e} be the curve which represents lines of constant N_e. In $\mathcal{M}_{A_3}$, γ_N uniformly bounds all inflationary trajectories with $N > N_e$. Define γ_∞ to be the curve specified by (IV.12).

Assume for the moment inflection point inflation takes place on $\mathcal{V}$. Since we are assuming uninformative — that is, constant — priors on $\mathcal{M}_{A_3}$, we can compute the likelihood of having *at least* N_e e-foldings of inflation by computing the area between the curves γ_{N_e} and γ_∞.

Using (VI.15), the area bounded between these curves is

$$\text{Area}_{N_e} = \lim_{A\to\infty}\int_0^A \frac{\pi^2}{8N_e^2\sqrt{3a}}\,da,$$

so that

$$\lim_{A\to\infty}\frac{\pi^2 A^{1/2}}{4\sqrt{3}N_e^2}. \tag{VI.16}$$

Just as with the Liouville measure, this quantity is divergent. Just as with the Gibbons-Turok approach, we will projectivize things. Suppose N_e is less than some fiducial number of e-foldings, $N_\star$. Then $\text{Area}_{N_\star} < \text{Area}_{N_e}$, and the likelihood of having at least N_e e-foldings relative to $N_\star$ is

$$\frac{\text{Area}_{N_e}}{\text{Area}_{N_\star}} = \left(\frac{N_\star}{N_e}\right)^2. \tag{VI.17}$$

Assuming inflection point inflation in a given universe $\mathcal{U}_{\text{inf}} \in \mathbb{M}$, the relative likelihood of having

precisely N_e e-foldings — relative to $N_\star$ is

$$\mathcal{P}(N_e|\mathcal{U}_{\rm inf}) \propto \lim_{\delta N\to 0}\left[\left(\frac{N_\star}{N_e}\right)^2 - \left(\frac{N_\star}{N_e-\delta N}\right)^2\right].$$

Therefore,

$$\boxed{\mathcal{P}(N_e|\mathcal{U}_{\rm inf}) \propto \left(\frac{N_\star}{N_e}\right)^3.} \tag{VI.18}$$

Two comments are in order. First, despite monotonic nature of each half γ_e about $b = 0$, the ratios of infinite areas may not be well-defined. Since α parametrizes this curve, these divergences correspond to the limits where $|\alpha| \to \infty$. As α is tied to the scale of inflation, it cannot be arbitrarily large.

Parameters like α should be bounded by the effective field theory cutoff, and it is precisely here that the ultraviolet physics would be invoked. However, if the ultraviolet physics were known, the statistical approach to the likelihood of inflation would be moot. Therefore, the cutoff supplied by A in (VI.16) is quite literally tied to our ignorance of the ultraviolet theory, and in the effective field theory case. Therefore, we continue with this simple regularization.

Second, this is a universal property of degenerate critical points. Since even slightly deformed inflection points are efficient attractors, the distinction between $\mathcal{U}_{\rm inf}$ and an arbitrary $\mathcal{U}$ in $\mathbb{M}$ will be exponentially close to fifty percent, independent of N, and can be incorporated in the overall normalization of the likelihood.

Given this fact, the result (VI.18) in remarkable agreement with recent Monte Carlo analyses which scanned over random potentials [14, 15]. In Ref. [14], D-brane inflation was investigated on the conifold, where up to six fields were employed! The emergence of a universal, inverse cubic scaling is easily explained in terms of (VI.18). In short, inflection point inflation dominates in these spaces of random potentials.

VI.5.3 Final Thoughts

By either standard, sixty e-foldings of inflation still appears unlikely. Whether or not these measures are the appropriate ones to impose on inflation is not the point of such an analysis. In [50] the point was that the initial conditions of inflation are not well understood. In [37] our point was not to negate this observation, but rather to show that allowing the Lagrangian itself to vary in the ensemble of possible universes leads to drastically different results.

CHAPTER VII

INFLECTION POINTS AND THE LARGEST SCALES

In this chapter we describe a specific application of the fixed point behavior of inflection point inflation to model an anomaly in the CMB data. We review the anomaly, perform the relevant computations and describe how inflection point inflation may best fit the data. This chapter is based on the worked first put forth in Ref. [38].

VII.1 An Anomaly in the CMB

We begin with a telegraphic discussion the angular power spectrum of temperature fluctuations in the CMB. During inflation, the nearly scale-invariant curvature perturbations expand rapidly until the reach horizon scales, at which time the "freeze". Because of the near vanishing mass of the inflaton during inflation, as now classical features in the spacetime metric, they do not decay. Rather, they lie in wait for the particle horizon to catch up as the universe proceeds with decelerated expansion. The radiation and matter that filled the universe subsequent to inflation now traverse the slightly featured landscape of spacetime. These perturbations had a direct effect on the thermal dynamics of the various constituents. In particular, during the era where the universe is filled with a plasma of baryons and electrons, it sourced perturbations between the oppositely charged fluids in what has become known as the **baryon acoustic oscillations** (BAO) of the early universe.

Just as the universe cooled to a point where the gas of photons no longer could efficiently strip electrons from nuclei, the surface of last scattering because a literal photograph of the quenching of this plasma. This photograph is the cosmic microwave background we observe today. In addition to the nearly scale-invariant background of thermal fluctuations, it also contains detailed information about the BAO. Therefore, the spectrum of temperature fluctuations in the CMB can be used to test astrophysical models of early universe dynamics.

One important definition is in order. The **angular power spectrum** is a Fourier transformation of the power spectrum on to the cosmic sphere, marginalized over the azimuthal directions. Concretely, it is the set of C_ℓ, where

$$C_\ell = \frac{2}{\pi}\int_0^\infty dk\, k^2 \mathcal{P}_{\mathcal{R}}(k) j_\ell(kr_\circ)^2.$$

In general, this expression is augmented to account for various astrophysical effects.

VII.1.1 Low Power at Large Scales

The angular power spectrum of thermal fluctuations in the CMB has a giant spike — and harmonic ringing — associated to the baryonic acoustic oscillations. The fundamental peak occurs at nearly $\ell \sim 200$, which corresponds to angular scales of one degree on the sky. These peaks occur on top of the scale-invariant background, which is flat and normalized by $\Delta^2_{\mathcal{R}}/2\ell(\ell+1)$. Since the background is flat, angular scales with $\ell < 100$ — scales before the peak — are predicted by inflationary theory to be approximately flat.

The data are not. a noticeable reduction of power at the largest scales ($\ell \sim 3$) was observed in WMAP, and a general trend of lower power through $\ell \sim \mathcal{O}(20)$ remained in the Planck analysis. Perturbations at these scales correspond to the earliest observable moments of inflation, a fact that can be used to attempt phenomenological explanations.

It is worth point out that the angular power spectrum has an intrinsic theoretical uncertainty at the largest scales. For each harmonic mode, $c_{\ell m}Y_{\ell m}$, the azimuthal modes, m are treated as independent observables. The theoretical uncertainty therefore scales[1] with ℓ as $1/\sqrt{(2\ell+1)^2}$, as we live in only one part of the universe. This theoretical limit of precision for the observed values of c_ℓ is known as **cosmic variance**.

Therefore, the low power observed at scales $\ell \lesssim 20$ may just be a statistical down fluctuation. The best hope for statistical significance of a CMB anomaly like this may be an improved global fit to all the cosmological data. This was attempted with the first year WMAP data [100] in Ref. [101], but no significant improvement was made. With the enhanced sensitivity of Planck — and the apparent enhancement of the anomaly — this issue is worth revisiting.

The origin of this anomaly has been studied before [101, 102, 103, 104, 105, 106], typically in the context of "just enough" inflation. In particular, if the inflaton dynamics are dominated by kinetic energy just before the minimum sixty or so e-foldings of inflation occur, the power spectrum could have a sharp suppression of power at the lowest scales as the system attracts towards the slow-roll trajectory. Inflection points offer a substantial generalization to this approach.

Inflection point inflation can extend the region of low power over a larger period of e-foldings as the field approaches the inflection point. It may therefore offer an explanation of not only the first few moments, but also the full Planck anomaly out to $\ell \sim \mathcal{O}(20)$. We now turn to a discussion of this phenomena.

VII.1.2 Deviations from Slow-Roll

Consider a single scalar field ϕ under the influence of an inflection point potential $\mathcal{V}$. For concreteness, this chapter will focus on the A_3 (quartic) model, familiar from (IV.13).

[1] Note that the errors associated to a two-point function measurement are inversely proportional to the number of measurements, rather than the inverse square-root.

Well above the inflection point, ϕ undergoes chaotic inflation (II.15), where

$$\phi(N) \propto \sqrt{\phi_i^2 - N}.$$

As ϕ approaches the inflection point, the dynamics much transfer to inflection point inflation, where performing the integral in (II.18) yields,

$$\phi(N) \propto \tan\left[\lambda_1\lambda_3(N_i - N)\right].$$

The actual solution ϕ interpolates between these two slow-roll approximations. The "full" slow-roll solution, $-\mathcal{V}_\phi/\mathcal{V}$, passes from a power law to a transcendental function, which requires a sharp reduction — including an inflection point in the graph of $\phi(N)$ — in field velocity near the inflection point in $\mathcal{V}$. This required "braking" is too much for the physical ϕ, and it bounces away sharply from the slow-roll trajectory just before inflection point inflation sets in. This can be quantified by a spike in the graph of $\Xi(N)$, defined in (II.30), shown explicitly in Fig. VII.1.

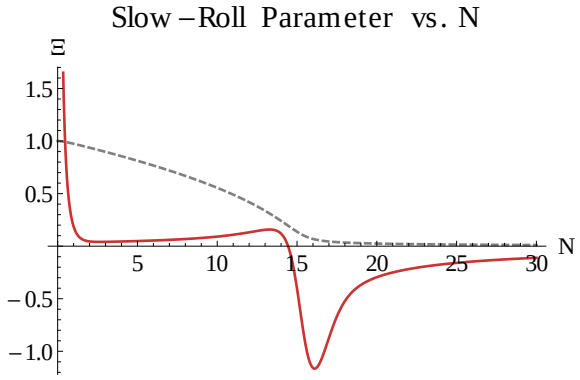

Figure VII.1: The slow-roll parameter Ξ versus N plotted for the cusp potential with $\alpha = 1$. ϕ starts from rest at $\phi = 10$. The field trajectory, $\phi/10$, is plotted for reference. The initial spike in Ξ comes from the deviation from the (non-vanishing) slow-roll trajectory. The chirp corresponds to the field breaking upon approach to the inflection point.

The magnitude of the spike in Ξ depends strongly on both the cubic coupling α and the initial conditions. Close to the boundary of the basin of attraction, the spike Ξ becomes $\mathcal{O}(1)$. Indeed, exponentially close to the boundary, it saturates at $\Xi = 3$. This is demonstrated in Fig. VII.2.

Recall that the power spectrum of density perturbations depends heavily on Ξ. Small Ξ is required to match observations. Large Ξ leads to a significant reduction in power, as just discussed. Therefore, if the inflection point affords only enough inflation to match observations — around sixty or so — then the spike in Ξ could explain the observed low power at angular scales less than $\ell \sim 20$. We make this connection precise in the next section.

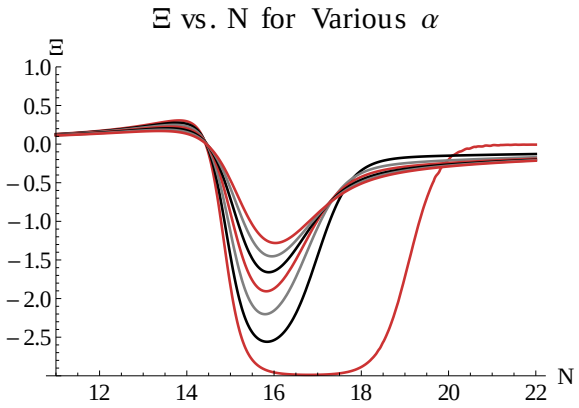

Figure VII.2: Variation of the slow-roll parameter spike, induced by the inflection point, with changing α. The largest spike corresponds to $\alpha = 0.661$, while the other curves decrease with decreasing α, in increments of 0.05.

VII.2 The Linear Perturbations

In this section we consider the effect of the inflaton "braking" as it transitions to inflection point inflation on the power spectrum. For concreteness, we focus on the A_3 potential,

$$\mathcal{V} = \frac{1}{4}\phi^4 + \alpha\phi^3 + \lambda\phi + \left(\frac{27}{4}\alpha^4 + 3\alpha\lambda\right).$$

The shape of the power spectrum defined in (II.40) depends strongly two parameters u and Ξ, defined in (**??**) and (II.30), respectively. Let us consider both of these in turn.

The u variable is essentially unity during slow roll inflation, as $\eta \propto -1/aH$, as argued in Section II.3.3. However, during the transition, this quantity spikes rapidly before settling back to unity. At first it might seem surprising, given that η and aH are both monotonic functions of N. Upon further inspection, one finds that u is essentially a ratio of two transcendental functions. Thus, such a behavior cannot be discounted. We illustrate this in Fig. VII.3.

We now turn to the behavior of ν. Recall that the spectral index is very sensitive to ν, as illustrated in Fig. II.1. ν also reacts strongly to the spike in Ξ as with the rest of the variables. For generic α, it then dips below unity for some time before slowly rising back above for a redshifted spectrum. This is shown in Fig. VII.4. The long transition shortens dramatically as α approach α_C or the initial conditions approach any other part on the basin of attraction. This is illustrated in Fig. VII.5

Plot and comment about the evolution of the power spectrum. Idea: if the transition occurs at the appropriate time, the low modes on the power spectrum will be blue shifted, but the higher modes will be redshifted? this effect can be quiet sharp or shallow, but this is a definite transition.

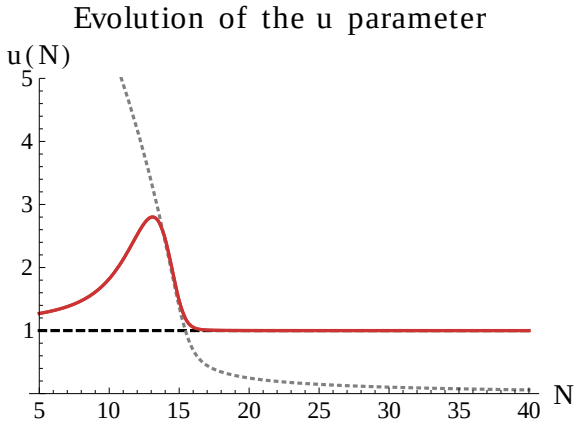

Figure VII.3: The u variable, defined in (II.38), plotted again N for slow-roll evolution . During de Sitter-like expansion u is near unity. The spike in this plot corresponds to the same jump away from slow-roll illustrated in Fig. VII.1. This trajectory started at rest from $\phi = 10$ in the A_3 potential with $\alpha = 1$ and $\lambda = 0.01$.

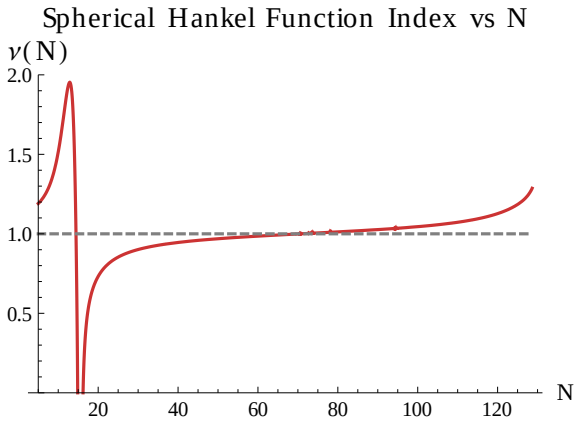

Figure VII.4: Effect of the deviation in slow roll near the inflection point on the Hankel Function index ν from Eqn. (II.39). The de Sitter case with unit ν is plotted for reference as a dashed line. Note the slow rise from a blueshifted spectrum to a redshifted one around $N = 80$. This trajectory started at rest from $\phi = 10$ in the A_3 potential with $\alpha = 1$ and $\lambda = 0.01$.

VII.3 Timing and the Angular Power Spectrum

VII.3.1 The Origin of the Anomaly

Finally we turn to these effects on the angular power spectrum. A flat spectrum — like the de Sitter case with $\nu = 1$ — leads to Fourier mode coefficients,

$$C_\ell = \frac{2}{\pi}\int_0^\infty dk\, \frac{j_\ell(kr_\circ)^2}{k} = \frac{1}{2\ell(\ell+1)}.$$

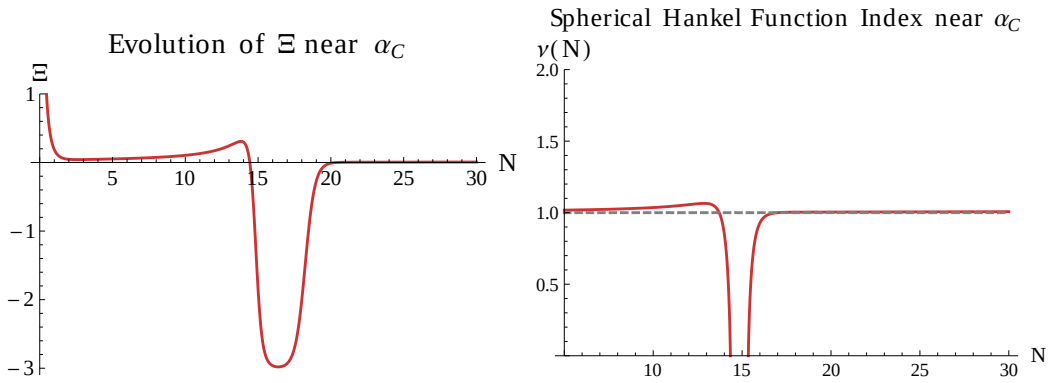

Figure VII.5: Behavior near α_C. Here the same system is shown, only with $\alpha = 0.659$ and $\lambda = 0.001$. On the left, the slow-roll parameter Ξ is plotted versus N. On the right, it is ν versus N. Notice the rapid exist of the blueshifted phase compared with that of $\alpha = 1$ in Fig. VII.4.

Here $r_\circ = 14$ Gpc is the comoving scale associated to the density perturbations relevant for the CMB. It has the important effect of allowing the approximation of the Hankel functions in $\Delta_{\mathcal{R}}$ by k^{1-n_s}.

For the de Sitter case, the plot of $\ell(\ell+1)C_\ell$ versus ℓ constant. Observations lead to a redshifted spectrum, with $n_s \sim 0.96$, which tilts this straight line slightly with a negative slope. On top of this nearly constant background, the effects of the BAO are included to give the CMB's power spectrum its familiar harmonic peaks.

The aforementioned CMB anomaly involves low power at large scale. The power in the first few C_ℓ is highly suppressed, and there is an aberration which continues nearly through to the first BAO peak. Assuming this is not a statistical aberration of cosmic variance — a significant assumption to be sure — this can happen only if the angular power spectrum is *blueshifted* for the first dozen ℓ, before returning to a slightly redshifted distribution at $\ell \sim \mathcal{O}(20)$.

From Section VII.2, we see that...

The fixed point dynamics of inflection point inflation gives a novel mechanism for the observed low power at large scales in the Cosmic Microwave Background.

Unlike previous investigations, [101, 102, 103, 104, 105], resolving this issue with inflection point inflation allows for shape and breadth (in ℓ) of the effect. While the use of inflection points for this effect was pointed out in [106], its full effect — particularly the strong enhancement near α_C — was not understood until the analysis in Ref. [38].

Assuming that the slow-roll phase of inflation occurs above the inflection point, the two parameters controlling the anomaly's effects are α and λ. Generally the full set of initial conditions can be considered, and the $\alpha \to \alpha_C$ enhancement occurs similarly near the boundary of the inflection point's basin of the attraction. Let us discuss the effects of α and λ in turn.

VII.3.2 Varying the Parameters

As previously discussed, low power at large scales amounts to a transition from a blueshifted spectrum to a redshifted at the largest angular scales — low values of ℓ. Since the modes are observed after reentering the horizon, the oldest observable perturbations are at the largest scales. If a transition to inflection point inflation is to account for this CMB anomaly, it must have happened just prior to the sixty or so e-foldings required by late-time cosmological observations. Therefore, in this scenario, the spectral index runs strongly with k at large scales.

Let us first estimate the duration of the relevant transition period, parametrized by N. Consider the modes that are significant for C_2 at N_i. As the universe expands, these modes appear to shrink. Suppose that at N_f, these modes are now observed at C_{200}. Coarsely, the number of e-foldings relevant for this change of scales — computed as arclengths on the celestial sphere — can be inferred from

$$\pi r_\circ e^{N_i} = \frac{\pi}{180} r_\circ e^{N_f} \Rightarrow N_f - N_i = \log 180,$$

suggesting that $N_f - N_i$ is just more than five. Thus, we are interested in the transitions in the Hankel function index, ν, from below to above unity on the scale of five e-foldings.

As α approaches α_C, the transition from a blueshifted spectrum to a redshifted one happens rapidly, which leads to a sharper transition over a shorter range of scales — alternatively, at earlier times. This is illustrated in Fig VII.6. It is notable that α parametrizes the class of A_3 models, and as discussed in Chapter IV, also sets the scale for a host of other physical quantities.

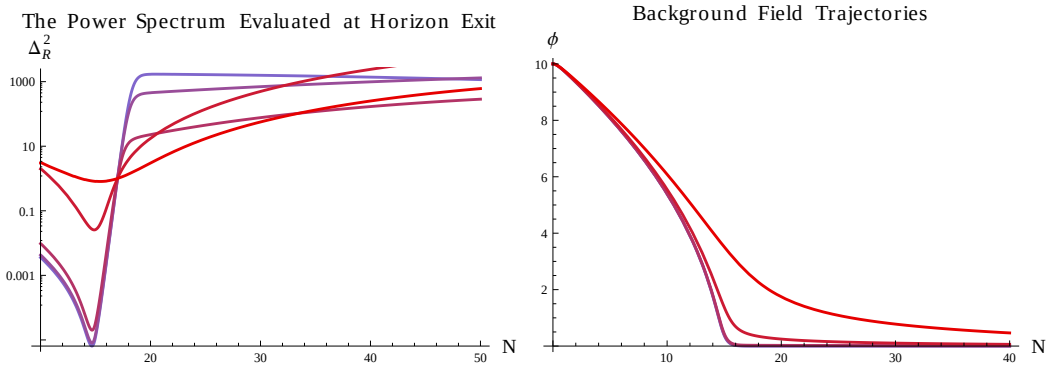

Figure VII.6: The power spectrum at horizon exit as a function of N is plotted on the left. On the right, the corresponding background field trajectories are presented. Each curve corresponds to a different $\alpha \in \{0.659, 0.665, 0.68, 1, 2\}$. λ was chosen to so that the initial conditions, $\phi = 10, \phi' = 0$ led an equal number of e-foldings, in this case 150. Colors range from blue to red respectively, and coordinate between the two plots. Three of the trajectory curves very nearly overlap. Note the large distortion caused by the transition to inflection point inflation.

$$C_\ell = \int_0^\infty dk k^2 \, \frac{\Delta^2_{\mathcal{R}}}{k^3} \, j_\ell(kr_\circ)^2.$$

$$\Delta^2_{\mathcal{R}} = \frac{k^3}{(a\phi')^2} \left| \frac{x}{\sqrt{2k}} h^{(1)}_\nu(x) \right|^3.$$

Recall that $x = k\Delta\eta = ku/aH$. Therefore,

$$\Delta^2_{\mathcal{R}} = \frac{k^3}{(a\phi')^2} \left| \frac{ku}{aH\sqrt{2k}} h^{(1)}_\nu(ku/aH) \right|.$$

Evaluated at horizon crossing, $k = aH$, so

$$\Delta^2_{\mathcal{R}} = \frac{(uk)^2}{2(a\phi')^2} \left| h^{(1)}_\nu(u) \right|.$$

Now, at horizon crossing

$$dk = d(aH) = aH \left(1 - \frac{1}{2}\phi'^2 \right) dN.$$

Notice that the limits coincide, *i.e.* $N(0) = 0$ and $N(\infty) = \infty$, at least in a quasi-de Sitter space. Therefore,

$$C_\ell = \int_0^\infty dN \, \left(1 - \frac{1}{2}\phi'^2 \right) \Delta^2_{\mathcal{R}} \frac{aH}{k} j_\ell(kr_\circ)^2,$$

so that that angular power spectrum may be finally written as

$$\boxed{C_\ell = \frac{1}{2} \int_0^\infty dN \, \frac{H^2 \left(1 - \frac{1}{2}\phi'^2 \right)}{\phi'^2} \, u^2 \left| h_\nu(u) \right| j_\ell(ar_\circ H)^2.} \tag{VII.1}$$

The spherical Bessel functions extract out the relevant parts of the power spectrum for the appropriate time scale associated to the angular scale on the sky. The integrand is vanishingly small before

$$ar_\circ H \sim \ell,$$

and the integral over the first dozen peaks or so are typically sufficient to give ninety-nine percent of the full integral. Note that N enters as an expectational here, so even for low ℓ these dozen peaks will occur within a few e-folds. The main point here is that the comoving distance to the surface of last scattering, $r_\circ$ sets the scale for these modes. In other words, the integrand is supported around

$$N - N_0 \sim \log(\ell / r_\circ H),$$

where N_0 sets the normalization of the scale factor. Given that u is extremely close to unity during inflation, (VII.1) is an incredibly simple expression. Indeed, from this expression it is easy to see how the deviations from unity observed in Fig. VII.3 source the disturbance observed in

Fig. VII.6. The effect on the angular power spectrum is illustrated in Fig. VII.7.

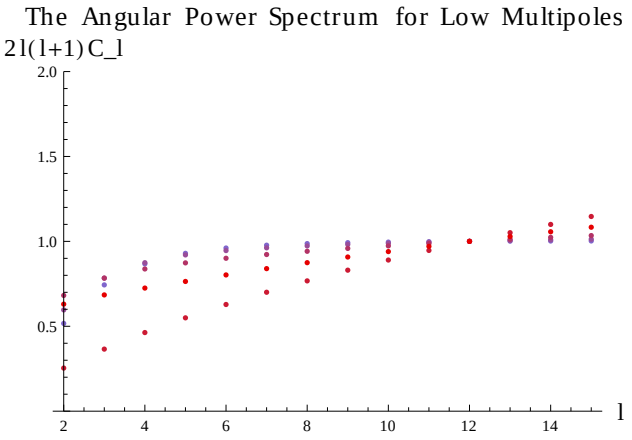

Figure VII.7: The lowest moments of the angular power spectrum are plotted. Each set of points is color coordinated with the those of Fig. VII.6, where the same data set was used. That is, α takes values in $\{0.659, 0.665, 0.68, 1, 2\}$, where color range from blue to dark red. Here, things are arranged so that $r_\circ aH$ is of order one at $N = 18$.

One comment is in order. Applying a time dependent formula such as (VII.1) implicitly assumes that the background on to which these perturbations — essentially random quantities — are being laid down is quite flat. In particular, no prior period of inflation, followed by a period of reentry has happened. Or, if it did happen, these ancient perturbations have somehow decayed so that a feature such as that seen in Fig. VII.6 might have been observed. Given what we know about the background dynamics this may not seem entirely unreasonable, although because H tends to decay with time, one might expect the power spectrum of such ancient perturbations to have a comparable normalization. While a mechanism for this might exist in some form of eternal inflation, we continue with the assumption that the perturbations are being laid down on a relatively flat background.

The duration of early period of blueshifted spectrum also depends on λ. From (II.19), one finds that very small λ leads to a large total number of e-foldings. If λ is too short, the blueshifted modes at the onset of inflection point inflation would not yet have reentered the horizon. If it were too small, sufficient inflation would not have occurred. Therefore, the range of λ required to explain the low power at large scales amounts to fortunate timing — to within five e-foldings or so — that we might be able to observe such an effect. Fig. VII.8 demonstrates the effect of varying λ on various values of α. While there is mild statistical degeneracy between the two parameters, it is clear from these figures that α determines the strength of the effect and λ determines is overall observability.

Given that the low modes of the angular power spectrum is subject to cosmic variance, such effects are best tested by examining the global fit to cosmological data. Given the results of

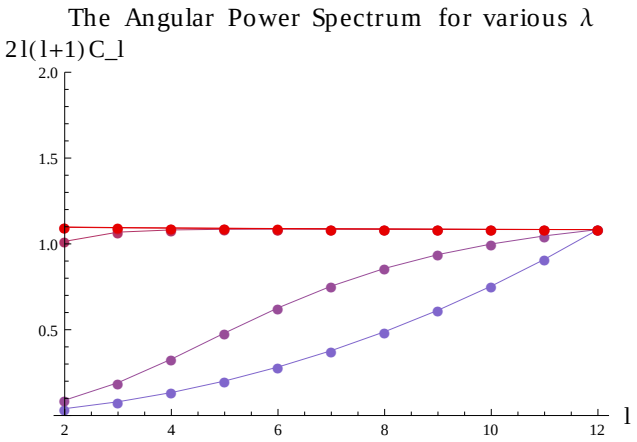

Figure VII.8: The lowest moments of the angular power spectrum are plotted with $\alpha = 0.659$ and $\lambda \in \{0.000324, 0.000305, 0.000286, 0.000270, 0.000255\}$, assuming the that $N_{CMB} = 60$. The sets of plotted modes are range from green to black. Notice how the effects shown in Fig. VII.7 dissipates with time.

Chapter IV, such a fit can be increased to include other specific details of the embedding of inflation into, for example, SUSY models of particle physics. We leave such a systematic analysis for future work.

CHAPTER VIII

CONCLUSION

VIII.1 Discussion

Physics beyond the standard model is a near certainty. Dark matter and dark energy were posited because of observations that do not fit within the known particle physics models or general relativity. These indirect observations compel us to search for new physics, but terrestrial experiments have had less than dramatic results. The LHC has observed a Higgs sector consistent with a minimal standard model, and the results of dark matter direct detection experiments have been inconclusive at best.

The thirty year old paradigm of weak scale supersymmetry is in ever increasing tension with observations and the gauge hierarchy problem has taken on renewed urgency. Without experimental guidance, the anthropic principle has resurfaced, and the possibility of a fine-tuned universe has become debatable point. The advent of precision cosmology has brought these problems into sharp relief.

Inflation has come to be the dominant paradigm for understanding the quantum theory behind the big bang. Its predicted, slightly redshifted spectrum of density perturbations has been observed and tied to both the cosmic microwave background and large scale structure. Despite this, there appears to be no distinguished manner in which the required scalar field condensate relates to known the known details of particle physics. Worse, there appears to be limitless possibilities for both the inflaton and the early universe which could give rise to our own whence, the anthropic debate.

While useful for matching to observations, effective field theory approaches to this problem cannot effectively determine the full, ultraviolet theory. Without knowledge of the fundamental Lagrangian and the symmetries it may possess — not to mention other new physical ideas — the observed universe is bound to look fined tuned. Without experimental guidance, we cannot pin down these symmetries or new ideas. Since the new Planck analysis suggests that our primordial universe is consistent with relatively anonymous single field, slow-roll scenario, the prospects for progress look bleak.

This dissertation blazes a new approach to early universe cosmology which embraces the vast number of possibilities. In Chapter IV, we reduced the study of the inflection point inflation scenario to a parametrized set of structural classes and studied their embeddings into various models of particle physics and string theory in Chapter V.

This approach has a curious duality. On the hand, it minimizes the details needed to study the physical consequences of the inflationary model in the low energy spectrum. On the other hand, it observes a fundamental limitation in what can be observed. For example, if our universe is re-

ally described by a complicated, KKLT-type model, observations gleaned from mirage mediation may point us towards the appropriate form of the scalar potential, but we will have little hope of understanding much about the ultraviolet details of the theory, *viz.* the nonperturbative D-brane effects or the SUSY breaking sector.

The utility of this approach becomes apparent when these quasi-universal properties applied to the study of inflation itself. In Chapter VI, we described the fixed point dynamics associated to inflection points. By expanding on previous studies of the measure problem in cosmology, we were able to show how inflection point inflation plays an important role once the couplings of the scalar potential are taken to be random variables. In the Gibbons-Turok construction [50] for example, the inflection point contribution was dominant. In any case, the fixed point behavior of inflection point inflation allowed for a $1/N^3$ scaling in the likelihood of having N e-foldings of inflation. This agrees well with recent monte carlo simulations of inflation on the conifold [14] and with random scalar potentials [15]. Finally, phenomenological applications of the fixed point dynamics were discussed in Chapter VII.

VIII.2 Future Investigations

There are a number of interesting avenues for further research, both theoretical and phenomenological. With respect to phenomenology, multifield dynamics offer a rich structure of observables. While the new Planck data excludes what many theorists expected, inflection point inflation produces a naturally low level — but not infinitesimal — level of "local" nongaussianity. It is entirely possible the more sensitive experiments will reveal such features, perhaps by probing the matter power spectrum. We are currently investigating the nongaussianity produced by ADE structural classes, and preliminary calculations demonstrate that different classes may yield different predictions for local nongaussianity. Similarly, other features of multifield models such as the possible creation of dangerous isocurvature perturbations may lead to new constraints on entire families of inflection point models.

Another interesting extension of this work would be a global fit of the inflection point solution to the low power anomaly to all the cosmological parameters. Additionally, this global fit can be extended to include particle physics searches, like the mirage mediation scenario discussed earlier. Since inflation can influence everything from baryogensis to reheating to nonthermal dark matter scenarios, there is an enormous opportunity to search for new correlations and constraints.

From a theoretical perspective, our study of the geometry of phase space opens many new lines of research. The Liouville measure has a natural ambiguity associated to the conformal version of Liouville's theorem valid in odd-dimensional phase spaces. Since the contact form associated to such spaces depends explicitly on the scalar potential, it is clear that a valid statistical measure on the set of possible trajectories much similarly depend on the scalar potential. A new approach to understanding the cosmological measure is required. Our approach of uninformative priors on the space of couplings is only a first step in this direction.

Canonical scalars lead naturally to slow-roll inflation. Non-canonical kinetic terms can similarly lead to an exponential expansion of space. This augments the attractor dynamics in Chapter VI. Trajectories similar in spirit to slow-roll inflation can exist, as seen in the DBI [21] and ghost inflation scenarios [22]. From a geometric perspective, one can interpret such "singular" trajectories as Legenderian singularities on phase space. The details of such singularities are known to be tightly restricted by the dimensionality of the contact manifold. Here, Arnold again supplies us with a classification scheme. It would be interesting to see if such classifications lead to classes with distinguishable but universal properties. While data suggests that single field slow roll inflation is favored, complete knowledge of these individual classes may offer an explanation as to why they are favored.

Without experimental guidance, early universe cosmology may find itself in the doldrums of anthropic reasoning. The main goal of this coarse-grainned approach to inflation is to isolate the main ideas behind the embedding of an early epoch quasi-de Sitter expansion within contemporary particle physics. This dissertation is but a step in this direction towards the proposal of entirely new ideas and experiments to test them.

[1] A. H. Guth, Phys. Rev. **D23**, 347 (1981).

[2] A. D. Linde, Phys. Lett. **B108**, 389 (1982).

[3] A. Albrecht and P. J. Steinhardt, Phys. Rev. Lett. **48**, 1220 (1982).

[4] A. G. Lemaître, Nature. **128**, 704 (1931).

[5] Particle Data Group, J. Beringer *et al.*, Phys.Rev. **D86**, 010001 (2012).

[6] M. R. Douglas and S. Kachru, Rev.Mod.Phys. **79**, 733 (2007), hep-th/0610102.

[7] F. Denef, p. 483 (2008), 0803.1194.

[8] E. Komatsu *et al.*, (2009), 0902.4759.

[9] Planck Collaboration, P. Ade *et al.*, (2013), 1303.5076.

[10] R. H. Brandenberger, (2012), 1203.6698.

[11] J.-L. Lehners, Phys.Rept. **465**, 223 (2008), 0806.1245.

[12] C. Burgess and L. McAllister, Class.Quant.Grav. **28**, 204002 (2011), 1108.2660.

[13] A. D. Linde and A. Westphal, JCAP **0803**, 005 (2008), 0712.1610.

[14] N. Agarwal, R. Bean, L. McAllister, and G. Xu, JCAP **1109**, 002 (2011), 1103.2775.

[15] J. Frazer and A. R. Liddle, JCAP **1202**, 039 (2012), 1111.6646.

[16] V. I. Arnol'd, *Singularity Theory* (Cambridge Unviersity Press, 1981), .

[17] A. A. Starobinsky, JETP Lett. **30**, 682 (1979).

[18] A. D. Linde, Phys.Lett. **B129**, 177 (1983).

[19] A. D. Linde, Phys.Rev. **D49**, 748 (1994), astro-ph/9307002.

[20] C. Armendariz-Picon, T. Damour, and V. F. Mukhanov, Phys.Lett. **B458**, 209 (1999), hep-th/9904075.

[21] M. Alishahiha, E. Silverstein, and D. Tong, Phys.Rev. **D70**, 123505 (2004), hep-th/0404084.

[22] N. Arkani-Hamed, P. Creminelli, S. Mukohyama, and M. Zaldarriaga, JCAP **0404**, 001 (2004), hep-th/0312100.

[23] X. Chen, Adv.Astron. **2010**, 638979 (2010), 1002.1416.

[24] J. M. Maldacena, JHEP **0305**, 013 (2003), astro-ph/0210603.

[25] D. H. Lyth and D. Wands, Phys.Lett. **B524**, 5 (2002), hep-ph/0110002.

[26] K. Enqvist and M. S. Sloth, Nucl.Phys. **B626**, 395 (2002), hep-ph/0109214.

[27] T. Moroi and T. Takahashi, Phys.Lett. **B522**, 215 (2001), hep-ph/0110096.

[28] N. S. Sugiyama, E. Komatsu, and T. Futamase, Phys.Rev. **D87**, 023530 (2013), 1208.1073.

[29] C. Cheung, P. Creminelli, A. L. Fitzpatrick, J. Kaplan, and L. Senatore, JHEP **0803**, 014 (2008), 0709.0293.

[30] S. Weinberg, Phys.Rev. **D77**, 123541 (2008), 0804.4291.

[31] D. Baumann, (2009), 0907.5424.

[32] S. Weinberg, *Cosmology* (Oxford University Press, Oxford, 2008).

[33] S. Weinberg, Phys.Rev.Lett. **59**, 2607 (1987).

[34] S. Downes, B. Dutta, and K. Sinha, Phys. Rev. **D84**, 063524 (2011), 1106.2266.

[35] R. Allahverdi, S. Downes, and B. Dutta, Phys.Rev. **D84**, 101301 (2011), 1106.5004.

[36] N. Itzhaki and E. D. Kovetz, Class.Quant.Grav. **26**, 135007 (2009), 0810.4299.

[37] S. Downes, B. Dutta, and K. Sinha, Phys.Rev. **D86**, 103509 (2012), 1203.6892.

[38] S. Downes and B. Dutta, (2012), 1211.1707.

[39] D. S. Salopek and J. R. Bond, Phys. Rev. **D42**, 3936 (1990).

[40] A. R. Liddle, P. Parsons, and J. D. Barrow, Phys. Rev. **D50**, 7222 (1994), arXiv:astro-ph/9408015.

[41] L. Kofman, *Physics of the Early Universe and Inflation* (Elsevier B.V., New York, 2007), .

[42] A. Vilenkin, Phys.Rev. **D27**, 2848 (1983).

[43] A. H. Guth, J.Phys. **A40**, 6811 (2007), hep-th/0702178.

[44] A. Aguirre, M. C. Johnson, and A. Shomer, Phys.Rev. **D76**, 063509 (2007), 0704.3473.

[45] WMAP Collaboration, E. Komatsu *et al.*, Astrophys.J.Suppl. **192**, 18 (2011), 1001.4538.

[46] L. McAllister and E. Silverstein, Gen.Rel.Grav. **40**, 565 (2008), 0710.2951.

[47] T. He, S. Kachru, and A. Westphal, JHEP **1006**, 065 (2010), 1003.4265.

[48] M. Cicoli and F. Quevedo, Class.Quant.Grav. **28**, 204001 (2011), 1108.2659.

[49] L. Kofman, A. D. Linde, and V. F. Mukhanov, JHEP **0210**, 057 (2002), hep-th/0206088.

[50] G. Gibbons and N. Turok, Phys.Rev. **D77**, 063516 (2008), hep-th/0609095.

[51] K. K. Wu, O. Lahav, and M. J. Rees, Nature **397**, 225 (1999), astro-ph/9804062.

[52] J. M. Bardeen, Phys.Rev. **D22**, 1882 (1980).

[53] R. L. Arnowitt, S. Deser, and C. W. Misner, Gen.Rel.Grav. **40**, 1997 (2008), gr-qc/0405109.

[54] A. Fialkov, N. Itzhaki, and E. D. Kovetz, JCAP **1002**, 004 (2010), 0911.2100.

[55] J. Ganc, Phys.Rev. **D84**, 063514 (2011), 1104.0244.

[56] J. Ganc and E. Komatsu, Phys.Rev. **D86**, 023518 (2012), 1204.4241.

[57] N. Agarwal, R. Holman, A. J. Tolley, and J. Lin, JHEP **1305**, 085 (2013), 1212.1172.

[58] S. R. Coleman, Phys.Rev. **D15**, 2929 (1977).

[59] J. Callan, Curtis G. and S. R. Coleman, Phys.Rev. **D16**, 1762 (1977).

[60] J. Alexandre and A. Tsapalis, Phys.Rev. **D87**, 025028 (2013), 1211.0921.

[61] J. M. Maldacena, Adv.Theor.Math.Phys. **2**, 231 (1998), hep-th/9711200.

[62] Supernova Search Team, A. G. Riess *et al.*, Astron.J. **116**, 1009 (1998), astro-ph/9805201.

[63] Supernova Cosmology Project, S. Perlmutter *et al.*, Astrophys.J. **517**, 565 (1999), astro-ph/9812133.

[64] O. Klein, Z.Phys. **37**, 895 (1926).

[65] W. Nahm, Nucl.Phys. **B135**, 149 (1978).

[66] F. Denef and M. R. Douglas, JHEP **0405**, 072 (2004), hep-th/0404116.

[67] F. Denef and M. R. Douglas, JHEP **0503**, 061 (2005), hep-th/0411183.

[68] S. Kachru, R. Kallosh, A. D. Linde, and S. P. Trivedi, Phys.Rev. **D68**, 046005 (2003), hep-th/0301240.

[69] S. Gukov, C. Vafa, and E. Witten, Nucl.Phys. **B584**, 69 (2000), hep-th/9906070.

[70] S. Kachru, J. Pearson, and H. L. Verlinde, JHEP **0206**, 021 (2002), hep-th/0112197.

[71] I. R. Klebanov and M. J. Strassler, JHEP **0008**, 052 (2000), hep-th/0007191.

[72] R. Kallosh and A. D. Linde, JHEP **0412**, 004 (2004), hep-th/0411011.

[73] J. Blanco-Pillado *et al.*, JHEP **0411**, 063 (2004), hep-th/0406230.

[74] C. Vafa, Nucl.Phys. **B469**, 403 (1996), hep-th/9602022.

[75] S. B. Giddings, S. Kachru, and J. Polchinski, Phys.Rev. **D66**, 106006 (2002), hep-th/0105097.

[76] S. Kachru, M. B. Schulz, and S. Trivedi, JHEP **0310**, 007 (2003), hep-th/0201028.

[77] O. DeWolfe, A. Giryavets, S. Kachru, and W. Taylor, JHEP **0507**, 066 (2005), hep-th/0505160.

[78] F. Denef, M. R. Douglas, and B. Florea, JHEP **0406**, 034 (2004), hep-th/0404257.

[79] E. Silverstein, Phys.Rev. **D77**, 106006 (2008), 0712.1196.

[80] M. R. Douglas, JHEP **1003**, 071 (2010), 0911.3378.

[81] T. Banks, (2012), 1208.5715.

[82] M. R. Douglas, (2012), 1204.6626.

[83] M. Reid, Math. Ann. **278**, 329 (1987).

[84] P. Candelas and X. C. de la Ossa, Nucl.Phys. **B342**, 246 (1990).

[85] S. R. Coleman and F. De Luccia, Phys.Rev. **D21**, 3305 (1980).

[86] P. Du Val, Mathematical Proceedings of the Cambridge Philosophical Society **30**, 453 (1934).

[87] R. Thom, *Structural stability and morphogenesis* (Addison Wesley Publishing Company, 1989).

[88] J. Martin, Mod.Phys.Lett. **A23**, 1252 (2008), 0803.4076.

[89] J. R. Ellis, J. Hagelin, D. V. Nanopoulos, K. A. Olive, and M. Srednicki, Nucl.Phys. **B238**, 453 (1984).

[90] T. Gherghetta, C. F. Kolda, and S. P. Martin, Nucl.Phys. **B468**, 37 (1996), hep-ph/9510370.

[91] I. Affleck and M. Dine, Nucl.Phys. **B249**, 361 (1985).

[92] R. Allahverdi, K. Enqvist, J. Garcia-Bellido, A. Jokinen, and A. Mazumdar, JCAP **0706**, 019 (2007), hep-ph/0610134.

[93] R. Allahverdi, B. Dutta, and K. Sinha, Phys.Rev. **D81**, 083538 (2010), 0912.2324.

[94] A. R. Liddle and D. Lyth, (2000).

[95] M. Henneaux, Lettere Al Nuovo Cimento Series 2 **38**, 609 (1983).

[96] G. Gibbons, S. Hawking, and J. Stewart, Nucl.Phys. **B281**, 736 (1987).

[97] S. Hawking and D. N. Page, Nucl.Phys. **B298**, 789 (1988).

[98] S. M. Carroll and H. Tam, (2010), 1007.1417.

[99] L. Jarv, T. Mohaupt, and F. Saueressig, JCAP **0408**, 016 (2004), hep-th/0403063.

[100] WMAP Collaboration, C. Bennett *et al.*, Astrophys.J.Suppl. **148**, 1 (2003), astro-ph/0302207.

[101] J. M. Cline, P. Crotty, and J. Lesgourgues, JCAP **0309**, 010 (2003), astro-ph/0304558.

[102] C. R. Contaldi, M. Peloso, L. Kofman, and A. D. Linde, JCAP **0307**, 002 (2003), astro-ph/0303636.

[103] D. J. Schwarz and E. Ramirez, p. 1241 (2009), 0912.4348.

[104] E. Ramirez, Phys.Rev. **D85**, 103517 (2012), 1202.0698.

[105] E. Dudas, N. Kitazawa, S. Patil, and A. Sagnotti, JCAP **1205**, 012 (2012), 1202.6630.

[106] R. K. Jain, P. Chingangbam, J.-O. Gong, L. Sriramkumar, and T. Souradeep, JCAP **0901**, 009 (2009), 0809.3915.

[107] F. Quevedo, S. Krippendorf, and O. Schlotterer, (2010), 1011.1491.

[108] V. T. Gurovich and A. A. Starobinsky, Sov.Phys.JETP **50**, 844 (1979).